

**A “suicide” BCG strain provides enhanced immunogenicity and robust protection against *Mycobacterium tuberculosis* in macaques**

Authors

Alexander A Smith<sup>1, 2\*</sup>, Hongwei Su<sup>3, 5\*</sup>, Joshua Wallach<sup>3\*</sup>, Yao Liu<sup>3</sup>, Pauline Maiello<sup>1, 2</sup>, H Jacob Borish<sup>1, 2</sup>, Caylin Winchell<sup>1</sup>, Andrew W Simonson<sup>1, 2</sup>, Philana Ling Lin<sup>2, 4</sup>, Mark Rodgers<sup>1, 2</sup>, Daniel Fillmore<sup>1, 2</sup>, Jennifer Sakal<sup>1, 2</sup>, Kan Lin<sup>3</sup>, Valerie Vinette<sup>3</sup>, Dirk Schnappinger<sup>3#</sup>, Sabine Ehrh<sup>3#</sup>, JoAnne L. Flynn<sup>1, 2#</sup>

<sup>1</sup> Department of Microbiology and Molecular Genetics, University of Pittsburgh School of Medicine, Pittsburgh PA

<sup>2</sup> The Center for Vaccine Research, University of Pittsburgh School of Medicine, Pittsburgh PA

<sup>3</sup> Department of Microbiology and Immunology, Weill Cornell Medicine, New York, NY 10021, USA.

<sup>4</sup> Department of Pediatrics, UPMC Children’s Hospital of Pittsburgh, University of Pittsburgh School of Medicine, Pittsburgh, PA

<sup>5</sup> Present address: Center for Veterinary Science, Zhejiang University, Hangzhou, China

\* These first authors contributed equally to this study

# These senior authors contributed equally to this study

**Abstract** (Limit: 150 words. Current: 150)

Intravenous (IV) BCG delivery provides robust protection against *Mycobacterium tuberculosis* (Mtb) in macaques but poses safety challenges. Here, we constructed two BCG strains (BCG-TetON-DL and BCG-TetOFF-DL) in which tetracyclines regulate two phage lysin operons. Once the lysins are expressed, these strains are killed in immunocompetent and immunocompromised mice yet induced similar immune responses and provided similar protection against Mtb challenge as wild type BCG. Lysin induction resulted in release of intracellular BCG antigens and enhanced cytokine production by macrophages. In macaques, cessation of doxycycline administration resulted in rapid elimination of BCG-TetOFF-DL. However, IV BCG-TetOFF-DL induced increased pulmonary CD4 T cell responses compared to WT BCG and provided robust protection against Mtb challenge,

with sterilizing immunity in 6 of 8 macaques, compared to 2 of 8 macaques immunized with WT BCG. Thus, a “suicide” BCG strain provides an additional measure of safety when delivered intravenously and robust protection against Mtb infection.

## Introduction

*Mycobacterium bovis* BCG, also known as Bacille Calmette-Guérin or BCG, is a live *Mycobacterium bovis* strain that was attenuated by serial passaging in vitro and remains the only tuberculosis (TB) vaccine approved for use in humans. BCG protects children against miliary TB and TB meningitis but is only partially protective against pulmonary TB <sup>1</sup>. Typically, BCG is delivered by intradermal injection, but studies in non-human primates revealed that endobronchial instillation or high-dose intravenous administration result in improved protection against *M. tuberculosis* (Mtb) infection <sup>2,3</sup>. Mucosal and intravenous delivery of BCG pose the risk of developing disseminated BCGosis, with potentially fatal outcomes in immunocompromised individuals <sup>4</sup>, such as HIV infected children <sup>5</sup>, children with Mendelian susceptibility to mycobacterial disease (MSMD) <sup>6</sup> and patients with chronic granulomatous disease <sup>7</sup>. Furthermore, intravesical BCG therapy is the most successful immunotherapy for bladder cancer but is also associated with severe and possibly fatal complications in approximately 5% - 8% of patients <sup>8-11</sup>.

We sought to construct a BCG strain that can be killed by addition or removal of a small molecule, such as a tetracycline <sup>12-14</sup> and would be safer than BCG so that it could be used with non-conventional delivery approaches and increased dosage. Mycobacteriophages use lytic enzymes to kill their host cells including holin proteins that permeabilize the cytoplasmic membrane, endolysins that cleave peptidoglycan and lipid hydrolases/esterases that degrade the outer membrane <sup>15</sup>. We took advantage of the lysin operons from the mycobacteriophages D29 and L5 <sup>16</sup> that encode a holin, an endolysin (lysin A) and a mycolylarabinogalactan esterase (lysin B) to construct regulated kill switches for BCG. We hypothesized that killing by inducing cell lysis may make BCG more immunogenic due to the release of intracellular antigens. In a previous study  $5 \times 10^7$  CFU of BCG (SSI strain) were delivered intravenously to rhesus macaques which resulted in substantial (~10,000 fold) reduction of live Mtb in the animals by 4 weeks, with 6 of 10 macaques showing sterile protection <sup>2</sup>. Here, we assessed whether doxycycline-controlled lysins can kill BCG (Pasteur strain) in mice and macaques. We evaluated the level of

60 persistence of BCG kill switch strains and the induced immune responses, and whether these strains  
61 administered intravenously could provide protection against Mtb challenge in mice and macaques.

## 62 Results

### 63 Construction and in vitro characterization of BCG kill switch strains

64 We evaluated the lysin operons of the mycobacteriophages L5 (L5L) and D29 (D29L) to construct BCG strains  
65 that could be efficiently killed by adding or removing tetracyclines such as anhydrotetracycline (atc) or  
66 doxycycline (doxy). We first tested functionality of these lysin operons in BCG using a TetON expression system  
67 <sup>12</sup>. Lysin transcription is repressed by a wild-type (WT) tetracycline repressor (TetR) that binds to a WT tetO  
68 positioned between the -10 and -35 elements of the lysin promoter. Addition of atc/doxy inactivates TetR and  
69 turns on lysin expression (**Fig. S1a**). As expected, atc addition prevented growth of BCG strains that carried  
70 TetON-D29L or TetON-L5L integrated into the chromosome, although escape mutants prevented complete  
71 killing and resulted in regrowth in liquid culture (**Fig1a, Fig. S1b**). The optical densities (OD) of BCG cultures  
72 carrying both TetON-D29L and TetON-L5L (BCG TetON-DL) rapidly declined when atc was added indicating  
73 that death occurred by cell lysis (**Fig. 1b, Fig. S2a**). The impact of atc on OD was similar regardless at what time  
74 after inoculation it was added. Cytosolic enolase and proteasome subunit B accumulated in the culture filtrate of  
75 BCG TetON-DL following treatment with atc, which demonstrated that atc-induced lysin expression indeed  
76 resulted in bacterial lysis (**Fig. S2b**). The combined induction of two lysins reduced the fraction of escape mutants  
77 by almost two orders of magnitude compared to those observed with single lysin strains (**Fig. S2c**).

78 To test whether L5L/D29L could also be used to generate atc/doxy-addicted BCG, which would require a  
79 tetracycline to grow, we cloned the lysin operons into two expression systems that are both silenced by atc/doxy.  
80 L5L was cloned into a TetPipOFF system <sup>17</sup>, in which WT TetR represses a second transcriptional repressor,  
81 PipR, that in turn represses L5L. Here, atc inactivates TetR, which turns lysin expression off via production of  
82 PipR. D29L was cloned into an expression system controlled by a reverse TetR (revTetR), which requires  
83 atc/doxy to efficiently bind to its operator DNA (tetO<sub>4C5G</sub>) <sup>13</sup>. Heterodimerization of TetR and revTetR produced  
84 in the same cell was prevented by using single-chain versions of each of these repressors <sup>18</sup>. Both BCG-TetOFF  
85 lysin strains were killed when atc was removed from the cultures (**Fig. 1c, Fig S2d**). The onset of killing was  
86 delayed compared to the TetON strains, which is likely due to the time required to dilute intracellular atc from the

87 bacteria. Death of the BCG-TetOFF strains was accompanied by cell lysis (**Fig. S2b**), and expression of two  
88 lysins led to enhanced killing and reduced the fraction of escape mutants (**Fig. S2e**). Analysis of the dual TetOFF  
89 lysin strain, BCG-TetOFF-DL, with fluctuation assays detected  $\sim 2 \times 10^{-9}$  escape mutants per cell division (**Fig.**  
90 **1d**).

### 91 **Lysin induction in intracellular BCG promotes proinflammatory cytokine production**

92 We infected bone marrow derived mouse macrophages (BMDM) with BCG and BCG-TetON-DL and treated  
93 them with rifampin (RIF) or atc (**Fig. 1e**). RIF killed both intracellular BCG and BCG-TetON-DL effectively. Atc  
94 had no effect on BCG but killed BCG-TetON-DL presumably via lysin induction. BCG and BCG-TetON-DL both  
95 induced TNF, IL12 p40 and IL-6 production by BMDMs. However, cytokine production was significantly increased  
96 when killing was mediated by phage lysin expression (**Fig. 1f-h**). These data suggest that intracellular lysis of  
97 BCG-TetON-DL enhanced cytokine production compared to that stimulated by live BCG or by BCG and BCG-  
98 TetON-DL that had been killed by RIF.

### 99 **Lysin induction kills BCG in immune competent and immune deficient mice**

100 In C57BL/6 mice BCG-TetON-DL established infection in lungs and spleens and persisted similar to BCG  
101 following intravenous injection (**Fig. 2 a,b**). When mice were treated with doxy starting seven days post infection,  
102 BCG-TetON-DL was killed in lungs and spleen, while doxy had a modest impact on WT BCG. BCG-TetOFF-DL  
103 similarly established infection in C57BL/6 mice that received doxy containing chow (**Fig. 2c,d**); its titers declined  
104 slowly in the lungs even when mice received doxy, likely due to doxy levels that were insufficient to maintain  
105 persistence in the context of host immunity, but remained stable in spleens. When doxy was eliminated from the  
106 mouse chow starting 14 days post infection, BCG-TetOFF-DL lost viability in lungs and spleens and was cleared  
107 from the lungs within 6 weeks of doxy withdrawal.

108 To assess safety of BCG-TetOFF-DL, we infected immunocompromised SCID mice (**Fig. 2c,d**). In SCID mice  
109 that received doxy, BCG-TetOFF-DL replicated in lungs during the 84 day-long infection. In spleens the strain  
110 replicated until it reached a titer of  $\sim 10^6$  and then persisted at a 10-fold higher burden than in C57BL/6 mice. In  
111 SCID mice that received doxy only for 14 days, BCG-TetOFF-DL was cleared from the lungs although slower  
112 than in immunocompetent C57BL/6 mice (**Fig. 2c**). In spleens, BCG-TetOFF-DL titers declined with kinetics like  
113 those observed in C57BL/6 mice (**Fig. 2d**). In a repeat experiment, BCG-TetOFF-DL was similarly eliminated

114 from lungs and declined in viability in spleens in SCID mice that received doxy for only 14 days (Fig. S3c).  
115 Although the strain replicated less in lungs of SCID mice that received doxy for 84 weeks than in the first  
116 experiment, the data reproducibly show that BCG-TetOFF-DL does not replicate in SCID mice in the absence of  
117 doxy. We assessed lung pathology and found rare, small cellular aggregates in both groups of mice without overt  
118 signs of disease (**Fig. S3d,e**). These data demonstrate that the dual lysin BCG kill switch strains recapitulate  
119 vaccination with BCG but can be killed by lysin expression via doxy administration or withdrawal. We have no  
120 evidence for the emergence of escape mutants in any of the animal experiments and BCG-TetOFF-DL proved  
121 to be safe in immunocompromised SCID mice.

### 122 **BCG kill switch strains provide similar protection as wild type BCG against Mtb infection in mice**

123 We vaccinated C57BL/6 mice by intravenous administration of  $1 \times 10^6$  BCG and BCG-TetOFF-DL and measured  
124 CFU in lungs and spleens 21, 56 and 84 days post vaccination (**Fig. S3a**). The mice did not receive any doxy,  
125 so that lysin expression was induced in BCG-TetOFF-DL soon after infection. Both strains lost viability in lungs,  
126 but BCG-TetOFF-DL was eliminated faster than BCG and cleared from the lungs by 56 days post vaccination.  
127 In spleens, BCG persisted at approximately  $2 \times 10^4$  CFU, while BCG-TetOFF-DL steadily lost viability, with 20  
128 CFU remaining on day 84.

129 We examined pulmonary T cell responses in vaccinated mice and in mice injected with PBS (**Fig. 3a-e**). BCG  
130 and BCG-TetOFF-DL elicited effector memory CD4 T cells (**Fig. 3a**) and CD8 T cells (**Fig. 3b**) whose frequencies  
131 were reduced on days 56 and 84 in BCG-TetOFF-DL vaccinated mice compared to BCG vaccinated mice.  
132 CD153 expressed on CD4 T cells has been identified as immune mediator of host protection against Mtb infection  
133 <sup>19,20</sup>. In mice vaccinated with BCG or BCG-TetOFF-DL, CD153 positive CD4 T cells were similarly enriched in  
134 the lungs on day 56 and 84 post vaccination (**Fig. 3c**). Lung resident memory CD4 T cells were also induced by  
135 vaccination, although the responses in mice vaccinated with BCG-TetOFF-DL were slightly lower than in mice  
136 vaccinated with BCG (**Fig. 3d**). Finally, we measured the frequency of pulmonary cytokine (TNF, IFN $\gamma$ , IL2,  
137 IL17A) expressing CD4 T cells and observed similar responses in BCG and BCG-TetOFF-DL vaccinated mice  
138 (**Fig. 3e**). Collectively these data indicate that vaccination with BCG-TetOFF-DL resulted in robust pulmonary T  
139 cell responses that were similar to those elicited by BCG vaccination, despite the absence of doxy from the  
140 beginning of vaccination and faster clearance of BCG-TetOFF-DL from the lungs (**Fig. S3a**).

141 We challenged unvaccinated and vaccinated mice with Mtb H37Rv via aerosol infection (**Fig. 3f**). Mtb H37Rv  
142 carried a hygromycin resistance cassette that allowed us to specifically detect Mtb in BCG and BCG-TetOFF-  
143 DL vaccinated mice. On day 28 post aerosol challenge, Mtb H37Rv had replicated to a mean of  $4 \times 10^6$  CFU in  
144 the lungs and  $2 \times 10^5$  CFU in the spleen of unvaccinated mice. In mice vaccinated with BCG or BCG-TetOFF-  
145 DL, the Mtb titers were reduced by approximately 10-fold ( $2.5 \times 10^5$ ) in lungs. In spleens BCG vaccination  
146 reduced Mtb burden by more than 100-fold compared to unvaccinated mice, while vaccination with BCG-  
147 TetOFF-DL led to a 30-fold reduction. We attribute this difference in protection to the significantly reduced  
148 persistence of BCG-Tet-OFF-DL compared to BCG in mouse spleens (**Fig. 2**). On day 56 post challenge, both  
149 BCG strains provided reduced protection against Mtb in lungs than on day 28, while levels of protection were  
150 largely maintained in the spleens. We repeated the challenge experiment with BCG-TetON-DL with similar  
151 outcomes although there was no difference in protective efficacy provided by BCG and BCG-TetON-DL in the  
152 spleens (**Fig. S4**). Together, these data demonstrate that BCG kill switch strains protect against Mtb infection in  
153 mice comparably to BCG, although they are eliminated more rapidly than BCG from lungs and spleens in the  
154 mouse model (**Fig. 2**).

### 156 **BCG persistence study design for NHPs**

157 We used BCG-TetOFF-DL to assess persistence in non-human primates. To determine whether the  
158 doxycycline-regulated lysin expression was functional in vivo in macaques and whether BCG-TetOFF-DL  
159 persisted or was diminished after removal of doxy treatment, we administered  $5 \times 10^7$  BCG-TetOFF-DL CFU IV  
160 to nine Mauritian cynomolgus macaques (MCM) (**Fig. 4a**). Group A was given daily doxy beginning one day prior  
161 to BCG inoculation and continued for 2 weeks and was euthanized at 4 weeks post-vaccination. Group B had  
162 the same 2-week doxy regimen and was euthanized at 8 weeks. Group C had an 8-week doxy regimen and was  
163 euthanized at 8 weeks. Doxy administration was expected to prevent the expression of the two lysin genes,  
164 maintaining the ability of BCG-TetOFF-DL to persist and/or grow in the macaques. Withdrawing doxy treatment  
165 after two weeks in groups A and B was expected to result in expression of the lysin genes, preventing replication  
166 or persistence of BCG-TetOFF-DL. Group C was maintained on doxy for the full 8 weeks of the study as a control  
167 group. We performed a bronchoalveolar lavage (BAL) 4 weeks post-vaccination. At necropsy, we plated tissues

168 for BCG-TetOFF-DL on plates containing atc. Single cell suspensions of BAL and tissue samples were assessed  
169 via flow cytometry for immune responses induced by BCG.

### 171 **BCG-TetOFF-DL induced robust T cell responses in airways**

172 After IV BCG-TetOFF-DL vaccination, the number of memory (CD45RA+CD28-, CD45RA-CD28+ or CD45RA-  
173 CD28-) CD4+ and CD8+ T cells recovered from the airways via BAL increased ~100-fold in all three groups,  
174 which is indicative of the generation of an IV BCG-dependent vaccine response, based on our previous studies  
175 <sup>2</sup> (**Fig. 4b**). This corresponded with an increase in the number of cytokine and cytotoxic molecule producing  
176 effector T cells in the BAL (**Fig. 4b**). Cell numbers and effector molecule expression between groups remained  
177 consistent, suggesting the duration of the doxy regimen and time of necropsy did not play a significant role in  
178 the generation of the immune response (**Fig 4h-i**). These data suggest that a BCG-dependent, multi-faceted,  
179 immune response was generated in all animal groups within 4 weeks post-vaccination. Stimulation with *M.*  
180 *tuberculosis* H37Rv whole-cell lysate did not have a large influence on the number of cytokine producing  
181 CD4+/CD8+ T-cells, when compared to unstimulated controls. This is likely due to the systemic spread of BCG-  
182 TetOFF-DL when administered via the intravenous route, resulting in common mycobacterial antigens persisting  
183 at this early time point post-vaccination.

### 185 **Cessation of doxycycline reduced BCG-TetOFF-DL bacterial burden in macaque tissues**

186 Gross pathology score is a quantitative measure of grossly apparent mycobacterial related lesions at necropsy.  
187 It takes into account granuloma numbers and lung lobes involved, lymph node and spleen size and granuloma  
188 involvement and any other evidence of infection <sup>21</sup>. Gross pathology scores (**Fig. 4c**) were relatively low in all  
189 groups, which was expected since the animals were not challenged with Mtb. Two animals in group A, and 1  
190 animal each in groups B and C had a few small granulomas found at necropsy, with 1 granuloma in a group A  
191 animal and 1 granuloma in a group B animal positive for BCG-TetOFF-DL CFU. BCG-TetOFF-DL bacterial  
192 burden was assessed in multiple tissue samples to assess the efficiency of the doxy dependent self-killing of the  
193 BCG-TetOFF-DL strain in all lung lobes, thoracic and peripheral lymph nodes and extrapulmonary organs  
194 (spleen and liver) of each animal (**Fig. 4d-g**). BCG-TetOFF-DL CFU was recovered at low levels from the lungs  
195 in 2 of 3 animals in group A (doxy stopped at 2 weeks and necropsied 4 weeks post-vaccination), from thoracic

lymph nodes of all 3 animals in group A, from peripheral lymph nodes in one animal and spleen from a different animal. For group B animals (necropsied at 8 weeks post BCG-TetOFF-DL which was 6 weeks post-doxycycline cessation), one was sterile (no CFU recovered), and BCG-TetOFF-DL was recovered from one lung sample in one animal and from the spleen in a different animal, all at low bacterial burdens. For group C animals (treated with doxy throughout the study and necropsied at 8 weeks post-BCG-TetOFF-DL), CFU were recovered from lung lobes in two animals and from a peripheral lymph node in two animals. No culturable bacteria were recovered from the blood at weeks 1 and 2 post vaccination or in the sternum, kidneys or liver of any animals. These data indicate that killing of BCG was accelerated when doxy treatment was stopped at 2 weeks post-vaccination. Group A (doxy treatment for 2 weeks, necropsied at 4 weeks) had a mean total body CFU of 479 (range 160-1041); Group B (doxy treatment for 2 weeks, necropsied at 8 weeks) mean total body CFU was 22 (range 0-50)(**Fig. 4d**). Group C (doxy for 8 weeks, necropsy at 8 weeks) had a mean total body CFU of 102 (range 25-195)(**Fig. 4d**). Thus, there was on average a 4.5-fold reduction in CFU ( $p=0.2$ , likely influenced by small sample size) in the animals that were treated with doxy for 2 weeks vs 8 weeks and necropsied at 8 weeks (i.e. comparing groups B and C). However, it is clear that even with continuation of doxycycline for the 8 weeks of this study (group C), BCG-TetOFF-DL bacterial burden was relatively low. This is consistent with our previous data on wild type SSI BCG <sup>2</sup>. Although the animals were vaccinated with  $>10^7$  CFU, BCG and BCG-TetOFF-DL appear to be rapidly reduced in macaques (~10,000 fold reduction by 8 weeks), suggesting minimal replication and/or enhanced bacterial killing.

Non-necrotizing ‘microgranulomas’ and lymphohistiocytic aggregates were seen throughout the spleen (**Fig. S5a**), thoracic lymph nodes (**Fig. S5b**) and livers (**Fig. S5c**) of animals in all groups. BCG-TetOFF-DL CFU was recovered from spleen in only 2/9 animals, liver in 0/9 animals and lymph nodes (peripheral or thoracic) in 6/9 animals.

### **Lymphocyte proportions in lung and lymph nodes were similar from each group post BCG-TetOFF-DL vaccination**

We compared lymphocyte composition in the lung and thoracic lymph nodes in tissue samples collected at necropsy (**Fig. S5d,e**). Expected levels of animal-to-animal variation was seen in cellular composition, however,



224 populations remained consistent within and across groups. CD4<sup>+</sup>CD8<sup>-</sup> (double negative) T cells were more  
225 prominent in group A lung tissues compared to group B and C, however other populations were similar. Few B  
226 cells (CD20<sup>+</sup>) were found in lung tissue compared to lymph nodes, but a higher proportion of  $\gamma\delta$  T-cells and NK  
227 cells were present in lung tissue. Cellular populations were similar across all animal groups in thoracic lymph  
228 nodes, with CD4<sup>+</sup> T-cells being the most prominent cell type.

### 229 230 **T-cell responses in the lung and lymph nodes at necropsy**

231 Comparing CD4<sup>+</sup> and CD8<sup>+</sup> T cell numbers in lung tissue at necropsy shows comparable levels of cells in all  
232 three groups (**Fig. 4h,i** – No stim). Similar cell numbers from animals on a short doxy regimen and necropsied  
233 at 4 weeks (Group A), and from those necropsied at 8 weeks (Group C) on a longer doxy regimen suggest a  
234 robust, multi-cellular immune response is generated and resides in the lungs within 4 weeks post vaccination  
235 with IV- BCG-TetOFF-DL. Cytokine and cytotoxic molecule producing cells were similar between all 3 groups,  
236 further reinforcing the multi-faceted response in lung tissue (**Fig. 4h,i**). A high number of CD4<sup>+</sup> cells responded  
237 to H37Rv whole cell lysate (WCL) stimulation, resulting in the production of TNF, IFN- $\gamma$  and IL-2 in the lung  
238 tissue. Cytotoxic molecules (granzyme B and K) are preformed molecules, therefore stimulation with H37Rv  
239 WCL has minimal effect on the quantities detected compared to unstimulated cells. High levels of these cytotoxic  
240 molecules were detected in all groups, in both unstimulated and stimulated samples.

241 In summary, IV BCG-TetOFF-DL vaccination was able to generate a robust, multi-faceted immune response  
242 comprising of effector CD4<sup>+</sup> and CD8<sup>+</sup> T-cells within 4 weeks post vaccination. The ‘kill-switch’ was successfully  
243 induced in a NHP model by removal of doxy, with a trend of reduction in BCG CFU 6 weeks after cessation of  
244 doxy administration. Gross pathology scores at necropsy remained low, suggesting minimal negative side-  
245 effects of IV BCG-TetOFF-DL vaccination.

### 246 247 **Determining protective efficacy of BCG-TetOFF-DL in macaques against Mtb infection and disease**

248 Following the persistence study, we performed an Mtb challenge study to assess the protective efficacy of BCG-  
249 TetOFF-DL and WT BCG Pasteur in NHPs. Protection was assessed by monitoring disease progression over  
250 time using PET-CT and quantifying Mtb bacterial burden at necropsy. The immune response generated to each

251 vaccine strain – BCG-TetOFF-DL and WT BCG Pasteur- was characterized over the duration of the study and  
252 at necropsy.

253 We administered  $5 \times 10^7$  BCG-TetOFF-DL or WT BCG Pasteur CFU to 8 MCMs per group, both intravenously  
254 (**Fig. 5a**). Two MCMs were unvaccinated as concurrent controls for this study; 8 additional historical  
255 unvaccinated MCM controls with the same time point for necropsy were included in this study, resulting in 10  
256 unvaccinated control MCMs total. To reduce the possibility of confounding effects, both vaccine groups were  
257 given a 2 week doxy regimen post-vaccination which should not affect WT BCG. At 22 weeks post vaccination,  
258 we challenged all groups with 9-16 CFU Mtb strain Erdman via intrabronchial instillation (**Fig. 5a**), monitored  
259 disease progression over time using PET/CT, and necropsied 12 weeks post-challenge.

### 261 **T-cell responses in airways were similar upon vaccination with BCG-TetOFF-DL or WT BCG Pasteur**

262 We monitored the immune response in the airways for both vaccine strains and unvaccinated control animals  
263 using BALs. BALs were performed pre-vaccination and 4, 12 and 20 weeks post IV-vaccination. We assessed  
264 the number of memory effector T-cells at each time point (memory CD4+ or memory CD8+ producing either IFN-  
265  $\gamma$ , TNF, IL-17, IL-2, GzmB, GzmK, granulysin or perforin) (**Fig. S6**). Both WT and BCG-TetOFF-DL induced a  
266 sustained increase in total T cell numbers in BAL while there was little change in the unvaccinated animals. This  
267 corresponded to a sustained increase in T cells producing cytokines and in CD8 T cells producing perforin in  
268 vaccinated animals. This confirms and extends our data from the persistence study (**Fig. 4**) that a robust T cell  
269 response is generated upon vaccination with both IV BCG-TetOFF-DL and WT BCG Pasteur. At 20 weeks, the  
270 final time point before challenge, we did not observe significant differences in effector T-cell numbers in the  
271 airway when comparing BCG-TetOFF-DL and WT BCG Pasteur. The similar level of response in both vaccination  
272 groups suggests live mycobacteria are only required to be present for a short amount of time for a robust memory  
273 response to be generated.

### 275 **BCG-TetOFF-DL and WT BCG had fewer granulomas and less lung inflammation compared to** 276 **unvaccinated macaques**

277 Serial PET-CT allows the assessment of disease trajectory by enumerating numbers of granulomas and lung  
278 and lymph node inflammation over time; increasing numbers of granulomas indicates Mtb dissemination which

279 correlates with development of active TB. Thus, greater the granuloma count, the more severe the infection and  
280 the less protective the vaccine. NHPs vaccinated with either BCG-TetOFF-DL or WT BCG Pasteur exhibited  
281 lower granuloma formation at every time point compared to unvaccinated control animals (**Fig. 5b,c**). One WT  
282 BCG Pasteur vaccinated NHP developed a large number of granulomas. Higher levels of the PET probe <sup>18</sup>F  
283 fluorodeoxyglucose (FDG) activity in the lung due to increased host cell glucose metabolism indicate an increase  
284 in lung inflammation <sup>21,22</sup>. We previously demonstrated that total lung FDG activity is correlated to bacterial  
285 burden in Mtb infected macaques <sup>2</sup>. Unvaccinated animals had significantly more total lung FDG activity after  
286 Mtb challenge compared to vaccinated animals (**Fig. 5d,e**). All animals of the BCG-TetOFF-DL vaccinated group  
287 had undetectable levels of inflammation (via lung FDG) just prior to necropsy, whereas 2 of the 8 animals in the  
288 WT BCG Pasteur group had elevated levels of total lung FDG activity (**Fig. 5e**).

### 290 **BCG-TetOFF-DL vaccination leads to enhanced protection against Mtb challenge**

291 At necropsy, gross pathology scores in vaccinated animals were significantly lower than unvaccinated animals  
292 (**Fig. 5f**). Our stated primary outcome measure of vaccine efficacy was total thoracic Mtb burden at necropsy.  
293 BCG-TetOFF-DL IV vaccinated animals displayed robust protection against Mtb with significantly lower total  
294 thoracic CFU compared to unvaccinated animals ( $p=0.001$ )(**Fig. 5g**). WT BCG IV vaccinated animals also had  
295 lower bacterial burdens compared to unvaccinated macaques ( $p=.0583$ )(**Fig. 5g**). Although BCG-TetOFF-DL  
296 was not significantly different than WT BCG in terms of total thoracic bacterial burden ( $p=0.3124$ ), 6 out of the 8  
297 animals in the IV-BCG-TetOFF-DL were sterile, defined as 0 Mtb CFU recovered, compared to two of eight for  
298 WT BCG (**Fig. 5h**). Thus, there was a trend towards increased sterile protection in the BCG-TetOFF-DL  
299 macaques (Fisher's exact test,  $p = 0.1319$ ). Total thoracic bacterial burden can be separated into lung CFU and  
300 thoracic lymph node (LN) CFU. BCG-TetOFF-DL vaccinated animals had significantly reduced lung CFU, with  
301 only one of the eight animals with lung CFU, while there was only a trend towards lower lung CFU in the WT  
302 BCG animals compared to unvaccinated animals (**Fig. 5i**). Both BCG-TetOFF-DL and WT BCG IV vaccinated  
303 animals had significantly lower thoracic LN CFU compared to unvaccinated animals (**Fig. 5j**), suggesting  
304 dissemination from lung to lymph nodes was reduced with both WT and BCG-TetOFF-DL.

## CD4 T cell responses are enhanced in the lungs of BCG-TetOFF-DL compared to WT BCG vaccinated

### macaques

The bacterial burden data suggest better protection by BCG-TetOFF-DL IV vaccination than by WT BCG using the Pasteur strain (6/8 sterile with BCG-TetOFF-DL vs 2/8 for WT BCG). To investigate the factors that might contribute to this, we analyzed immune cell populations and functions in the tissues of the macaques at necropsy. Multiparametric spectral flow cytometry and Boolean gating revealed a significantly higher frequency of CD4<sup>+</sup> T cells in lungs of BCG-TetOFF-DL animals, whereas the CD8<sup>+</sup> T cell population was slightly, although not significantly, higher in WT BCG Pasteur vaccinated animals (**Fig. 6a**). There was a significant increase in the frequency of lung memory CD4<sup>+</sup> T-cells producing cytokines (IFN- $\gamma$ , TNF, IL-17 and/or IL-2) in the BCG-TetOFF-DL vaccinated group compared to the WT BCG Pasteur group upon stimulation with mycobacterial WCL (**Fig. 6b**). There were no statistically significant differences between BCG-TetOFF-DL or WT BCG vaccinated animals in lung T cells producing cytotoxic effector molecules, although slightly higher frequencies were seen in WT BCG vaccinated animals (**Fig. 6b**). In the thoracic lymph nodes, WT BCG vaccinated animals had significantly higher frequencies of CD8<sup>+</sup> T cells producing cytotoxic molecules compared to BCG-TetOFF-DL vaccinated animals (**Fig. 6d**). There was an increase in the number of cytokine producing memory CD4<sup>+</sup> cells, specifically IFN- $\gamma$ , IL-2 and TNF, present in the lung tissue of BCG-TetOFF-DL vaccinated macaques compared to those vaccinated with WT BCG (**Fig. S7**), corroborating the significant increase in frequency of CD4 T cells.

### Spleen pathology

Due to the systemic nature of IV BCG vaccination and the robust immune response induced, splenomegaly was observed in NHPs<sup>2</sup>. The duration of the enlargement and the relationship with BCG survival is unknown. Here we show that spleen size appears to correlate with time post-vaccination and BCG CFU (**Fig. S8**). IV-BCG vaccinated and IV-BCG vaccinated/Mtb challenged animals had spleen sizes that were larger than the average range of an unvaccinated/unchallenged macaque but were largest at 4 weeks post vaccination. Spleen size reduced over time, with the smallest measurement being recorded 34 weeks post vaccination. Even spleens from unvaccinated but Mtb challenged macaques did not fall within the normal range. We assume that this is due to Mtb infection in these animals, noting that IV BCG vaccinated and Mtb challenged animals had spleen sizes similar to unvaccinated and challenged macaques at this late time point.

334

## 335 Discussion

336 BCG has likely been administered to more humans than any other vaccine designed to prevent infectious  
337 diseases and is generally safe <sup>23</sup>. Though rare (0.1 to 4.3 per one million vaccinated children), complications  
338 from, BCG vaccination is one of the most common causes of death in immunocompromised children <sup>24</sup>. Although  
339 BCG is an effective option for treatment of bladder cancer, approximately 8% of patients develop complications  
340 which leads to cessation of treatment <sup>11</sup>. We therefore sought to generate BCG strains whose elimination does  
341 not depend on a patient's immune system. Usage of phage lysins to establish conditional kill switches was  
342 prioritized over other toxins because we expected these enzymes to not only increase safety but to also increase  
343 immunogenicity via the release of cytoplasmic antigens.

344

345 Combining the controlled expression of two phage lysins resulted in BCG strains that either require atc/doxy to  
346 grow or are efficiently killed by exposure to atc/doxy and escape from this controlled growth was as low as  $\sim 2 \times$   
347  $10^{-9}$  mutants per cell division. Escape was thus not as low as for the Mtb strain described in the accompanying  
348 manuscript (Wang et. al. submitted) but likely low enough to allow studies in humans given that BCG is  
349 attenuated already. Characterization of the atc/doxy-addicted BCG (BCG-TetOFF-DL) in SCID mice confirmed  
350 that induction of lysin expression is sufficient to eliminate the strain from the lungs and reduce bacterial burden  
351 in the spleens in the absence of an intact immune system. Mice vaccinated with BCG-TetOFF-DL or WT BCG  
352 showed similar protection against Mtb challenge, even though the BCG-TetOFF-DL strain was eliminated faster  
353 than WT BCG. It seems likely that protection benefited from lysis of BCG-TetOFF-DL as it releases additional  
354 antigens. This interpretation is supported by the enhanced stimulation of proinflammatory cytokines we observed  
355 in macrophages infected with this strain compared to WT BCG.

356

357 BCG delivered intravenously was shown to provide robust protection against Mtb infection and disease in  
358 macaques <sup>2,25</sup>. Here we show, using genetically modified BCG that is killed by cessation of doxy administration  
359 in vivo in macaques, that BCG does not need to be alive for more than a few weeks to provide robust protection  
360 against Mtb challenge. Our data indicate that this "suicide" BCG strain induces greater CD4 T cell responses in

361 lungs and may provide even more robust protection than WT BCG in macaques. Using a self-killing BCG strain  
362 may thus increase the safety of IV BCG vaccination strategies while maintaining remarkable protective efficacy.

363  
364 The ability of BCG-TetOFF-DL to generate a robust CD4 response could be vital in its ability to be an efficacious  
365 vaccine, as CD4 T cells are known to play an important role in protection against TB <sup>26</sup>. Our data indicated that  
366 BCG-TetOFF-DL induces a stronger CD4 T cell response compared to WT BCG with production of key cytokines  
367 including IFN- $\gamma$  and TNF in lungs. We hypothesize that the lysis of BCG-TetOFF-DL leading to release of  
368 mycobacterial proteins and the enhanced cytokine production by macrophages, as shown in vitro, leads to a  
369 more robust priming of T cells in vivo, at least in macaques.

370  
371 BCG IV was previously noted to result in enlarged spleens in macaques. We considered that reducing the  
372 duration of live BCG could mitigate this side effect. In the persistence study, at 4 weeks post-BCG-TetOFF-DL,  
373 spleens were quite large, but reduced in size by 8 weeks. Spleen sizes were smaller overall in the BCG-TetOFF-  
374 DL vaccinated macaques that received doxy for only 2 weeks compared to those receiving doxy for 8 weeks. In  
375 the Mtb challenged animals, both vaccinated and unvaccinated animals had increased spleen sizes compared  
376 to “normal” spleens and were slightly smaller than the spleens harvested at 8 weeks post-vaccination, although  
377 spleen size can vary with age, sex, and size of macaques. Mtb infection generates immune responses resulting  
378 in spleen enlargement, which may suggest the normal spleen size range is not achievable in Mtb infected groups  
379 <sup>27</sup>. The BCG associated non-necrotizing ‘microgranulomas’ that were present 4- and 8-weeks post-vaccination  
380 were not seen in animals necropsied at 34 weeks post-vaccination.

381  
382 BCG-TetOFF-DL was generated using a BCG Pasteur background and the WT BCG used as a comparator here  
383 was the same Pasteur strain, while our previous IV-BCG studies performed in NHPs used BCG-SSI (Danish) as  
384 the vaccine strain <sup>2,25,28</sup>. Thus, both BCG Pasteur and BCG Danish/SSI can achieve sterilizing levels of protection  
385 when delivered IV. This study and one other BCG IV study <sup>28</sup> were performed in Mauritian cynomolgus macaques  
386 (MCM) while our original study was performed in rhesus macaques. MCM have similar susceptibility to TB  
387 disease as rhesus macaques <sup>21,29</sup> and BCG IV provides robust protection in both macaque <sup>2,25,28</sup>. In contrast,  
388 BCG-TetOFF-DL or WT BCG delivered IV provided only modest protection in mice in the current study, similar

389 to other studies with IV BCG in mice <sup>30,31</sup>. Thus, vaccines that provide robust protection in macaques cannot  
390 always be predicted from murine data.

391  
392 Limitations to this study are the small samples sizes used in the macaque persistence study which limited  
393 statistical analyses. Similarly, larger sample sizes for the macaque protective efficacy study could provide clearer  
394 differences between BCG-TetOFF-DL and WT BCG outcomes. Future studies could also assess whether doxy  
395 is necessary in vivo, or whether the strain could be eliminated even earlier in the vaccination phase. In mice it  
396 remains to be demonstrated whether vaccination efficacy can be improved by prolonging persistence of the BCG  
397 kill switch strain by administrating doxy for different periods of time.

398  
399 The safety and efficacy of IV-BCG in humans is yet to be determined and there are practical challenges to  
400 implementing BCG IV for widespread vaccination. One concern is the increased spleen sizes in macaques  
401 following BCG IV and whether the systemic spread of live-attenuated bacteria may result in human illness. The  
402 “suicide” strain developed in this study aimed to resolve some of these issues, while maintaining the high levels  
403 of protection seen with WT IV-BCG vaccination. Although the splenomegaly was still present, spleen size did  
404 reduce over time. We did not observe any adverse effects or signs of illness in the macaques following WT or  
405 BCG-TetOFF-DL vaccination, and blood cultures during the early phase of vaccination were negative. In our  
406 previous study in SIV+ macaques given WT BCG, blood cultures were also negative 2 weeks post-vaccination  
407 <sup>28</sup>.

408  
409 In summary, our data support that a limited exposure to BCG delivered intravenously is effective against Mtb  
410 challenge. The use of a strain that lyses itself may provide enhanced protection due to increased immunogenicity  
411 in vivo. This “suicide” BCG strain could limit safety concerns that are raised regarding IV administration of a live  
412 vaccine as well as provide an option for safer intradermal BCG vaccination of immunocompromised individuals  
413 and treatment for bladder cancer.

414

## 415 **Materials and Methods**

416 **Strains, media and culture conditions.** All *M. bovis* BCG strains are derived from BCG Pasteur TMC 1011  
417 obtained from the American Type Culture Collection (ATCC #35734). *M. tuberculosis* H37Rv was used for  
418 challenge experiments. Strains were cultured in liquid Middlebrook 7H9 medium supplemented with 0.2%  
419 glycerol, 0.05% tween80 and ADN (0.5% bovine serum albumin, 0.2% dextrose, 0.085% NaCl) and on  
420 Middlebrook 7H10 agar plates supplemented with 0.5% glycerol and Middlebrook OADC enrichment (Becton  
421 Dickinson). Antibiotics were added for selection of genetically modified strains at the following concentrations:  
422 hygromycin (50 µg/ml), kanamycin (25 µg/ml), zeocin (25 µg/ml). Anhydrotetracycline was used at 0.5 or 1 µg/ml.

423 **Generation of strains.** To create the TetON single and dual-lysin strains, BCG was transformed with either or  
424 both plasmids pGMCK3-TSC10M1-D29L and pGMCgZni-TSC10M1-L5L, integrating the D29-lysin and L5-lysin  
425 into BCG L5 and Giles sites, respectively. To create the TetOFF single and dual-lysin strains, BCG was  
426 transformed with either or both plasmids pGMCK3-TSC10M-TsynC-pipR-SDn-P1-TsynE-PptR-L5L and  
427 pGMCgZni-TSC38S38-TrrnBd2-P749pld-10C32C8C-D29L, integrating the L5-lysin and D29-lysin into BCG L5  
428 and Giles sites, respectively. The single lysin strains were cultured in the presence of 0.5 µg/ml atc and the dual  
429 lysin strain was cultured in the presence of 1 µg/ml atc.

430 **Analysis of bacterial lysis by immunoblotting.** Culture filtrates were prepared as follows. BCG strains were  
431 grown in 7H9 medium with 0.2% glycerol, 0.05% Tween-80, 0.5% BSA, 0.2% dextrose and 0.085% NaCl until  
432 the culture reached an OD of 0.6 ~ 0.8. Cultures were then washed three times with PBS to remove BSA and  
433 Tween-80. We next suspended the pellet in 7H9 medium supplemented with 0.2% glycerol, 0.2% dextrose and  
434 0.085% NaCl. After incubation, culture supernatant was harvested by centrifugation and filtration through 0.22  
435 µm filters. Filtrates were concentrated 100-fold by using 3K centrifugal filter units (Millipore) and analyzed by  
436 immunoblotting with antisera against Eno and PrcB.

437 **Fluctuation analysis.** Fluctuation analysis was performed as previously reported<sup>32</sup>. Briefly, BCG strains were  
438 inoculated at permissive condition (1.0 µg/mL atc) in 7H9 media supplemented with OADC in the presence of  
439 antibiotics (20 µg/mL kanamycin, 25 µg/mL zeocin). After reaching OD=1.0, the culture was diluted to multiple  
440 4-mL aliquots with 1,000 bacteria. The diluted culture was grown for 11-14 days in 7H9+OADC media in  
441 permissive conditions in the presence of antibiotics. Once OD was at 1.0, bacteria were washed for three times



442 and resuspended in 400  $\mu$ L 7H9+OADC without atc. Four aliquots of bacteria were streaked onto 7H10+OADC  
443 plates supplemented with antibiotics (20  $\mu$ g/mL kanamycin, 25  $\mu$ g/mL zeocin) and 1.0  $\mu$ g/mL atc for bacteria  
444 count, and the rest aliquots were spread onto 7H10+OADC plates with antibiotics (20  $\mu$ g/mL kanamycin, 25  
445  $\mu$ g/mL zeocin) and either atc, or no atc. According to Ma, Sarkar, Sandri (MSS) method<sup>33</sup>, the estimated number  
446 of mutations per culture ( $m$ ) was inferred by number of mutant ( $r$ ) colonies observed on plates. The escape rate  
447 was calculated by dividing  $m$  by  $N_i$ , the number of cells plated for each culture. The Mann-Whitney  $U$  test was  
448 used to statistically compare escape rates between two groups. The lowest detection limit was calculated based  
449 on an assumption that only one colony could be observed in all 20 independent cultures.

450 **Preparation and infection of murine bone marrow derived macrophages (BMDMs).** Femurs and tibias of  
451 female C57BL/6 mice were extracted, and bone marrow cells were aseptically flushed using PBS. Cells were re-  
452 suspended in Dulbecco's modified eagle medium (DMEM) supplemented with 10% fetal bovine serum (FBS)  
453 and 20% L929 culture filtrate and incubated for 6 days to allow differentiation into macrophages. Cells were  
454 harvested and seeded at  $6 \times 10^4$  per well in 96-well plates in DMEM supplemented with 10% FBS, glycine and  
455 10% L929 cell culture overnight before infection. Mycobacteria were washed in PBS + 0.05% tyloxapol and a  
456 single cell suspension was generated by low-speed centrifugation to pellet clumped cells. The bacteria were  
457 diluted into DMEM, 10% LCM and added to macrophages at MOI of 0.1. After 4 hours, extracellular bacteria  
458 were removed by washing the macrophages three times with warm PBS. Infected BMDMs were treated with atc  
459 (0.5  $\mu$ g/ml) or RIF (0.5  $\mu$ g/ml) starting 16 hrs post infection. Cytokines were quantified using BD OptEIA ELISA  
460 kits for mouse TNF, IL-12p40 or IL6 (BD Biosciences). The number of intracellular bacteria was determined by  
461 lysing macrophages with 0.01% Triton X-100 and culturing dilutions of macrophage lysates on 7H10 agar plates.

462 **Mouse infections.** Female 8- to 10-week-old C57BL/6 (# 000664, Jackson Laboratory) were vaccinated with ~  
463  $10^6$  CFU of the indicated BCG strain by the intravenous route. Mice received doxycycline containing mouse chow  
464 (2,000 ppm; Research Diets) for the indicated periods. Mice were infected with Mtb H37Rv using an inhalation  
465 exposure system (Glas-Col) with a mid-log phase Mtb culture to deliver approximately 100 bacilli per mouse. To  
466 enumerate CFU, organs were homogenized in PBS and cultured on 7H10 agar. Charcoal (0.4 %, w/v) was added  
467 to the plates that were used to culture homogenates from doxy treated mice. Agar plates were incubated for 3-  
468 4 weeks at 37°C. Mice were housed in a BSL3 vivarium. All mouse experiments were approved by and performed  
469 in accordance with requirements of the Weill Cornell Medicine Institutional Animal Care and Use Committee.

**Flow cytometry to assess immune responses in mice.** Mouse lungs were isolated and placed in RPMI1640 containing Liberase Blendzyme 3 (70 µg/ml; Roche) and DNase I (50 µg/ml; Sigma-Aldrich). Lungs were then cut into small pieces and incubated at 37 C for 1 hour. The cells were filtered using cell strainers, collected by centrifugation, resuspended in ACK hemolysis buffer (ThermoFisher) and incubated for 10 minutes at room temperature. Cells were then washed with PBS and resuspended in splenocyte medium (RPMI-1640, supplemented with 10% FBS, 2 mM GlutaMax 10 mM HEPES, and 50 µM 2-mercaptoethanol). For intracellular staining samples, cells were stimulated with PPD (20 µg/ml) in the presence of anti-CD28 antibody (37.51, BioLegend) for 1.5 hours and 10 µg/ml Brefeldin A (Sigma) and monesin were added and incubated at 37 C for another 3 hrs. Samples were kept on ice in a refrigerator overnight. Cells were stained with Zombie-NIR (BioLegend) to discriminate live and dead cells. Purified anti-CD16/32 antibody (93, BioLegend) was used to block Fc receptor before staining. PerCp-Cy5.5 anti-CD62L (MEL-14, Thermofisher), BV605 anti-CD4 (RM4-5, BioLegend), BV711 anti-CD8 (53-6.7, BioLegend), eFluor450 anti-CD11a (M17/4, Thermofisher), BUV395 anti-CD153 (RM153, BD Biosciences), BV480 anti-CD69 (H1.2F3, BD Biosciences), APCC7 anti-CD44 (IM7, BioLegend) were used to stain cells for 30 minutes at room temperature. The cells were fixed in fixation buffer (BioLegend) for 30 minutes and taken out of BSL3. The cells were incubated for 20 minutes in permeabilization buffer (eBioscience) before intracellular cytokine staining. BV421 anti IL-17A (TC11-18H10.1, Biolegend), BV750 anti-IFN $\gamma$  (XMG1.2, BD Biosciences), PE-C5.5 anti-IL-2 (JES6-5H4, Biolegend), FITC anti-TNF (MP6-XT22, BioLegend), BV785 anti-CD3 (17A2, BioLegend) were used to stain cells for 30 minutes. Cells were washed and resuspend in cell staining buffer (BioLegend). Flow cytometry data were acquired on cytometer (LSR Fortessa TM; BD Biosciences) or cytometer (Cytek Aurora; Cytek Biosciences) and were analyzed with FlowJoTM V10.

## **Macaques**

Mauritian cynomolgus macaques (*Maccaca fascicularis*) used in this study were obtained from BioCulture US (all males, 6-9 years old). All procedures and study design complied with ethical regulations and were approved by the Institutional Animal Care and Use Committee of the University of Pittsburgh. Macaques were housed either singly or in pairs in a BSL2 animal facility and cared for in accordance with local, state, federal, and institute policies in facilities accredited by the American Association for Accreditation of Laboratory Animal Care (AAALAC), under standards established in the Animal Welfare Act and the Guide for the Care and Use of Laboratory Animals. During the Mtb challenge phase, animals were housed in a BSL3 animal facility. Macaques

were monitored for physical health, food consumption, body weight, temperature, complete blood counts, and serum chemistries. Full details on macaques in this study are in **Table S3**.

### **BCG vaccination**

To assess persistence of BCG-TetOFF-DL, animals that were intravenously vaccinated were sedated with ketamine (10 mg/kg) or telazol (5- 8 mg/kg) and injected intravenously with  $3.74 \times 10^7$  CFU BCG-TetOFF-DL vaccine in an injection volume of 1mL. Animals that underwent challenge with *M. tuberculosis* strain Erdman were vaccinated intravenously with  $5 \times 10^7$  CFU BCG-TetOFF-DL or WT BCG Pasteur.

### **Macaque Mtb challenge**

Macaques were challenged by bronchoscope with 9-16 Mtb strain Erdman 22 weeks post vaccination as previously described<sup>34</sup>. Control animals (unvaccinated) were challenged at the same time. Historical control unvaccinated and Mtb challenged MCMs (previously published by our group<sup>28</sup>) were included for statistical analyses and comparison.

### **Blood, BAL and tissue processing**

To assess the presence of viable BCG-TetOFF-DL, blood was drawn from each animal 1- and 2-weeks post vaccination. Blood was cultured and the presence of BCG-TetOFF-DL assessed using atc-containing plates. Bronchoalveolar lavages for the persistence study in macaques were performed pre-vaccination, 4 weeks post vaccination (all groups) and 8 weeks post vaccination (for groups B and C). For the immunization and challenge studies in macaques, BAL was performed prior to vaccination and monthly thereafter until the time of challenge. Procedures were performed as previously described<sup>2</sup>. PBMCs were isolated from peripheral blood using Ficoll-Paque PLUS gradient separation (GE Healthcare Biosciences) and standard procedures.

### **PET/CT**

PET/CT scans were performed at designated time points throughout the study to assess thoracic cavity inflammation. Animals were sedated with 10 mg/kg ketamine / 0.5 ml atropine before imaging. An intravenous catheter was placed in the saphenous vein and animals were injected with ~ 5 millicurie (mCi) of <sup>18</sup>F-FDG. Once placed on the imaging bed, anesthesia was induced with 2.5 to 3% isoflurane which is reduced to 0.8–1.2% for

524 maintenance. Breathing during imaging was maintained using an Inspiration 7i ventilator (eVent Medical, Lake  
525 Forest, CA, USA) with the following settings: PF = 9.0 l/min, respiration rate = 18–22 bpm, tidal volume = 60 ml,  
526 O<sub>2</sub> = 100, PEEP = 5–8 cm H<sub>2</sub>O, peak pressure = 15–18 cm H<sub>2</sub>O, I:E ratio = 1:2.0. A breath hold was conducted  
527 during the entirety of the CT acquisition.

528 PET/CT scans were performed on a MultiScan LFER 150 (Mediso Medical Imaging Systems, Budapest,  
529 Hungary). CT acquisition was performed using the following parameters: Semi-circular single field-of-view, 360  
530 projections, 80 kVp, 670  $\mu$ A, exposure time 90 ms, binning 1:4, voxel size of final image: 500 x 500  $\mu$ m. PET  
531 acquisition was performed 55 min after intravenous injection of <sup>18</sup>F-FDG with the following parameters: 10 min  
532 acquisition, single field-of-view, 1–9 coincidence mode, 5 ns coincidence time window. PET images were  
533 reconstructed with the following parameters: Tera-Tomo 3D reconstruction, 400–600 keV energy window, 1–9  
534 coincidence mode, median filter on, spike filter on, voxel size 0.7 mm, 8 iterations, 9 subsets, scatter correction  
535 on, attenuation correction based on CT material map segmentation. Serial CT or PET/CT images were acquired  
536 pre-infection and at 4 and 11 dpi. Animal A2 was CT scanned at 9 dpi instead of 11 dpi, and animal A1 was  
537 scanned at 18 dpi in addition to the standard imaging schedule previously described.

538 Images were analyzed using OsiriX MD or 64-bit (v.11, Pixmeo, Geneva, Switzerland). Before analysis, PET  
539 images were Gaussian smoothed in OsiriX and smoothing was applied to raw data with a 3 x 3 matrix size and  
540 a matrix normalization value of 24. Whole lung FDG uptake was measured by first creating a whole lung region-  
541 of-interest (ROI) on the lung in the CT scan by creating a 3D growing region highlighting every voxel in the lungs  
542 between -1024 and -500 Hounsfield units. This whole lung ROI was copied and pasted to the PET scan and  
543 gaps within the ROI were filled in using a closing ROI brush tool with a structuring element radius of 3. All voxels  
544 within the lung ROI with a standard uptake value (SUV) below 1.5 were set to zero and the SUVs of the remaining  
545 voxels were summed for a total lung FDG uptake (total inflammation) value. Thoracic lymph nodes were analyzed  
546 by measuring the maximum SUV within each lymph node using an oval drawing tool. Both total FDG uptake and  
547 lymph node uptake values were normalized to back muscle FDG uptake that was measured by drawing cylinder  
548 ROIs on the back muscles adjacent to the spine at the same axial level as the carina (SUV<sub>CMR</sub>; cylinder-muscle-  
549 ratio). PET quantification values were organized in Microsoft Excel and graphed using GraphPad Prism.

## 550 **Necropsy, pathology scoring, BCG burden and Mtb burden**

551 At necropsy, NHPs were sedated with ketamine and had a maximal blood draw then euthanized by sodium  
552 pentobarbital injection, followed by gross examination for pathology. A gross pathology scoring system was  
553 employed, assessing lung, lymph node and extrapulmonary compartments <sup>21</sup>. Spleen size was also measured.  
554 Average spleen size of adult macaques was provided by the Wisconsin Primate Center. A pre-necropsy PET-  
555 CT scan was used to map lesions in the thoracic cavity and at necropsy these regions were excised and  
556 homogenized to form a single-cell suspension. Uninvolved lung tissue, lymph nodes and spleen were also  
557 processed. To recover BCG-TetOFF-DL, the individual cell suspensions were plated on 7H11 agar + atc and  
558 incubated at 37°C with 5% CO<sub>2</sub> for 3 weeks with atc replenished on the plates after 10 days of incubation. CFU  
559 were counted to assess the BCG-TetOFF-DL burden of each animal. To assess Mtb burden post-challenge,  
560 single-cell suspensions were plated on 7H11 agar and incubated at 37°C with 5% CO<sub>2</sub> for 3 weeks.

## 561 **Multiparameter flow cytometry**

562 Up to one million viable cells isolated from tissue or BAL were stimulated with 20 µg/ml H37Rv Mtb whole cell  
563 lysate (WCL) (BEI Resources), 1 µg/ml each of ESAT-6 and CFP-10 peptide pools (provided by Aeras, Rockville,  
564 MD) or R10 media for 2 h before adding 10 µg/ml BD GolgiPlug (BD Biosciences) for a further 12 hours. Cells  
565 were surface stained to allow for the assessment of cell composition, followed by intracellular staining (ICS) for  
566 the analysis of cytokine and cytotoxic molecule production. Permeabilization for ICS was performed using BD  
567 Fixation/Permeabilization Kit. Surface and ICS antibody cocktails were made in BD Brilliant Stain buffer. Cells  
568 were analyzed using a five laser Cytek® Aurora spectral flow cytometer. The flow cytometry results were  
569 analyzed using FlowJo™ v10.8 Software (BD Life Sciences). All antibodies used in the flow panels are shown  
570 in **Table S1** and **Table S2**. Gamma/delta (TCR106, Invitrogen) and perforin (3465-3-500, Mabtech) antibodies  
571 were conjugated with PE/Cy5® Conjugation Kit (ab102893, abcam) and Alexa Fluor® 488 Conjugation Kit -  
572 Lightning-Link® (ab236553, abcam) respectively. Gating strategy is presented in **Fig. S9**.

## 573 **Statistical methods**

574 For mice, generation of graphics and data analyses were performed in Prism version 10.0.2 software  
575 (GraphPad). NHP data were tested for normality using the Shapiro-Wilk test. For comparisons between only  
576 BCG-TetOFF-DL and WT, Mann-Whitney tests were used. For comparisons including historical unvaccinated

577 macaque controls, Kruskal-Wallis tests were performed and Dunn's p-values (adjusted for multiple comparisons)  
578 were reported. For longitudinal data with only 3 animals per group, two-way repeated measure ANOVA was  
579 performed (random variable was NHP) with the assumption of sphericity. For BAL longitudinal data, groups  
580 were compared at each time point using unpaired t-tests (with Welch correction) and Holm-Šídák adjustment for  
581 multiple comparisons. For categorical variables, Fisher's exact test p-value was reported. Statistical tests were  
582 not run for any groups with 3 or fewer points. All p-values less than 0.10 are shown.

## 584 **Data Availability Statement**

585 All relevant data are available from the corresponding author upon reasonable request.

## 587 **Acknowledgements**

588 We thank Eric Rubin, Sarah Fortune, Kristine Guinn at Harvard University and Robert A. Seder, Patricia Darrah  
589 and Mario Roederer at the NIH for helpful discussions. We thank Rodrigo Aguilera Olvera, Heather Kim and  
590 Anthony Castro for help with the mouse infection studies. We thank Sophie Lavalette-Levy, Anisha Zaveri and  
591 Natalie Thornton for their help with cloning and data analysis. We thank Erica Larson and Chuck Scanga for  
592 providing historical macaque control data. We are grateful to the veterinary and research technicians in the Flynn  
593 lab for their dedication and expertise in conducting these studies. Research reported in this publication was  
594 supported by NIH R01 AI143788, by Leidos Biomedical Research Inc and the National Cancer Institute of the  
595 NIH under Contract Number HHSN2612015000031 and NIH NIAID Contract 75N93019C00071. The content is  
596 solely the responsibility of the authors and does not necessarily represent the official views of Leidos Biomedical  
597 Research, Inc. or the National Institutes of Health.

## 599 **References**

- 600 1. Trunz, B.B., Fine, P. & Dye, C. Effect of BCG vaccination on childhood tuberculous meningitis and miliary  
601 tuberculosis worldwide: a meta-analysis and assessment of cost-effectiveness. *Lancet* **367**, 1173-80  
602 (2006).
- 603 2. Darrah, P.A. *et al.* Prevention of tuberculosis in macaques after intravenous BCG immunization. *Nature*  
604 **577**, 95-102 (2020).
- 605 3. Dijkman, K. *et al.* Disparate Tuberculosis Disease Development in Macaque Species Is Associated With  
606 Innate Immunity. *Front Immunol* **10**, 2479 (2019).
- 607 4. Yamazaki-Nakashimada, M.A., Unzueta, A., Berenise Gamez-Gonzalez, L., Gonzalez-Saldana, N. &  
608 Sorensen, R.U. BCG: a vaccine with multiple faces. *Hum Vaccin Immunother* **16**, 1841-1850 (2020).

5. Hesseling, A.C. *et al.* The risk of disseminated Bacille Calmette-Guerin (BCG) disease in HIV-infected children. *Vaccine* **25**, 14-8 (2007).
6. Jouanguy, E. *et al.* Interferon-gamma-receptor deficiency in an infant with fatal bacille Calmette-Guerin infection. *N Engl J Med* **335**, 1956-61 (1996).
7. Conti, F. *et al.* Mycobacterial disease in patients with chronic granulomatous disease: A retrospective analysis of 71 cases. *J Allergy Clin Immunol* **138**, 241-248 e3 (2016).
8. Alexandroff, A.B., Jackson, A.M., O'Donnell, M.A. & James, K. BCG immunotherapy of bladder cancer: 20 years on. *Lancet* **353**, 1689-94 (1999).
9. Gonzalez, O.Y. *et al.* Spectrum of bacille Calmette-Guerin (BCG) infection after intravesical BCG immunotherapy. *Clin Infect Dis* **36**, 140-8 (2003).
10. Kawai, K., Miyazaki, J., Joraku, A., Nishiyama, H. & Akaza, H. Bacillus Calmette-Guerin (BCG) immunotherapy for bladder cancer: current understanding and perspectives on engineered BCG vaccine. *Cancer Sci* **104**, 22-7 (2013).
11. Liu, Y., Lu, J., Huang, Y. & Ma, L. Clinical Spectrum of Complications Induced by Intravesical Immunotherapy of Bacillus Calmette-Guerin for Bladder Cancer. *J Oncol* **2019**, 6230409 (2019).
12. Ehrt, S. *et al.* Controlling gene expression in mycobacteria with anhydrotetracycline and Tet repressor. *Nucleic Acids Res* **33**, e21 (2005).
13. Kim, J.H. *et al.* A genetic strategy to identify targets for the development of drugs that prevent bacterial persistence. *Proc Natl Acad Sci U S A* **110**, 19095-100 (2013).
14. Klotzsche, M., Ehrt, S. & Schnappinger, D. Improved tetracycline repressors for gene silencing in mycobacteria. *Nucleic Acids Res* **37**, 1778-88 (2009).
15. Catalao, M.J. & Pimentel, M. Mycobacteriophage Lysis Enzymes: Targeting the Mycobacterial Cell Envelope. *Viruses* **10**(2018).
16. Ford, M.E., Sarkis, G.J., Belanger, A.E., Hendrix, R.W. & Hatfull, G.F. Genome structure of mycobacteriophage D29: implications for phage evolution. *J Mol Biol* **279**, 143-64 (1998).
17. Boldrin, F. *et al.* Development of a repressible mycobacterial promoter system based on two transcriptional repressors. *Nucleic Acids Res* **38**, e134 (2010).
18. Krueger, C., Berens, C., Schmidt, A., Schnappinger, D. & Hillen, W. Single-chain Tet transregulators. *Nucleic Acids Res* **31**, 3050-6 (2003).
19. Du Bruyn, E. *et al.* Mycobacterium tuberculosis-specific CD4 T cells expressing CD153 inversely associate with bacterial load and disease severity in human tuberculosis. *Mucosal Immunol* **14**, 491-499 (2021).
20. Sallin, M.A. *et al.* Host resistance to pulmonary Mycobacterium tuberculosis infection requires CD153 expression. *Nat Microbiol* **3**, 1198-1205 (2018).
21. Maiello, P. *et al.* Rhesus Macaques Are More Susceptible to Progressive Tuberculosis than Cynomolgus Macaques: a Quantitative Comparison. *Infect Immun* **86**(2018).
22. White, A.G. *et al.* Analysis of 18FDG PET/CT Imaging as a Tool for Studying Mycobacterium tuberculosis Infection and Treatment in Non-human Primates. *J Vis Exp* (2017).
23. Lange, C. *et al.* 100 years of Mycobacterium bovis bacille Calmette-Guerin. *Lancet Infect Dis* **22**, e2-e12 (2022).
24. Hassanzad, M., Valinejadi, A., Darougar, S., Hashemitari, S.K. & Velayati, A.A. Disseminated Bacille Calmette-Guerin infection at a glance: a mini review of the literature. *Adv Respir Med* **87**, 239-242 (2019).
25. Darrah, P.A. *et al.* Airway T cells are a correlate of i.v. Bacille Calmette-Guerin-mediated protection against tuberculosis in rhesus macaques. *Cell Host Microbe* **31**, 962-977 e8 (2023).
26. Sakai, S., Mayer-Barber, K.D. & Barber, D.L. Defining features of protective CD4 T cell responses to Mycobacterium tuberculosis. *Curr Opin Immunol* **29**, 137-42 (2014).
27. Chapman, J., Goyal, A. & Azevedo, A.M. Splenomegaly. in *StatPearls* (Treasure Island (FL), 2024).
28. Larson, E.C. *et al.* Intravenous Bacille Calmette-Guerin vaccination protects simian immunodeficiency virus-infected macaques from tuberculosis. *Nat Microbiol* **8**, 2080-2092 (2023).
29. Rodgers, M.A. *et al.* Preexisting Simian Immunodeficiency Virus Infection Increases Susceptibility to Tuberculosis in Mauritian Cynomolgus Macaques. *Infect Immun* **86**(2018).
30. Mittrucker, H.W. *et al.* Poor correlation between BCG vaccination-induced T cell responses and protection against tuberculosis. *Proc Natl Acad Sci U S A* **104**, 12434-9 (2007).
31. Pym, A.S. *et al.* Recombinant BCG exporting ESAT-6 confers enhanced protection against tuberculosis. *Nat Med* **9**, 533-9 (2003).

- 664 32. Ford, C.B. *et al.* Mycobacterium tuberculosis mutation rate estimates from different lineages predict  
665 substantial differences in the emergence of drug-resistant tuberculosis. *Nat Genet* **45**, 784-90 (2013).  
666 33. Rosche, W.A. & Foster, P.L. Determining mutation rates in bacterial populations. *Methods* **20**, 4-17  
667 (2000).  
668 34. Martin, C.J. *et al.* Digitally Barcoding Mycobacterium tuberculosis Reveals In Vivo Infection Dynamics in  
669 the Macaque Model of Tuberculosis. *mBio* **8**(2017).  
670

671  
672  
673  
674  
675  
676  
677  
678  
679  
680  
681 **Figure 1. Induction of phage lysins results in cell lysis with low frequency of escape and promotes**  
682 **macrophage proinflammatory cytokine production.**

683 (a) Growth of BCG TetON single and dual lysin kill switch strains with and without atc. Individual CFU data points  
684 from two replicate cultures are depicted.

685 (b) Impact of BCG TetON dual lysin kill switch induction at different times of growth.

686 (c) Growth of BCG TetOFF single and dual lysin kill switch strains with and without atc. Data are means  $\pm$  SD  
687 from triplicate cultures. Error bars are frequently too small to be seen.

688 (d) Fraction of resistant mutants per culture and mutation rate per cell division of BCG-TetOFF-DL. The  
689 resistance rate in 20 individual cultures was determined in a fluctuation assay. The number of mutations per cell  
690 division was calculated using the bz-rates web-tool.

691 (e) CFU quantification of WT BCG and BCG-TetON-DL (plus or minus atc or rifampin) during infection of murine  
692 BMDMs. Data are means  $\pm$  SD from triplicate cultures. Multiple unpaired t-tests were performed on  $\log_{10}$ -



transformed data comparing BCG-TetON-DL treated with rif to BCG-TetON-DL treated with atc at each time point with Holm-Šídák adjusted p-values. \*  $p < 0.05$ , #  $0.05 < p < 0.10$ .

(f, g, h) Quantification of TNF (f), IL-12 p40 (g), and IL-6 (h) production by macrophages infected with BCG or BCG-TetON-DL and treated with rifampin or atc for 20 hrs. Data are means  $\pm$  SD from triplicate cultures. Significance was determined by one-way ANOVA with Tukey's adjusted p-values. \*\*\*\*  $p < 0.0001$ , \*\*\*  $p < 0.001$ , \*\*  $p < 0.01$ , \*  $p < 0.05$ , ns  $p > 0.1$ . ND, not detected.

All data are representative of two or three independent experiments.

**Figure 2. Phage lysin induction kills BCG in immune competent and immune deficient mice.** (a, b) CFU quantification from lungs (a) and spleens (b) of BCG and BCG-TetON-DL infected C57BL/6 mice treated or not with doxycycline (doxy) starting day 7 post infection. Data are means  $\pm$  SD from 3-5 mice per group and time point. (c, d) CFU quantification from lungs (c) and spleens (d) of BCG-TetOFF-DL infected C57BL/6 and SCID mice treated or not with doxy for the indicated times. Data are means  $\pm$  SD from 4-5 mice per group and time point. Multiple unpaired t-tests run on  $\log_{10}$ -transformed data at each time point with Holm-Šídák adjusted p-values shown comparing BCG with BCG + doxy (black p-values), BCG-TetON-DL with BCG-TetON-DL + doxy (purple p-values), BCG-TetOFF-DL with BCG-TetOFF-DL + doxy in C57BL/6 (blue p-values) and in SCID (red p-values) mice.

**Figure 3. BCG-TetOFF-DL and wt BCG provide similar protection against Mtb infection in mice.** Mice were i.v. vaccinated with BCG or BCG-TetOFF-DL or received PBS.

(a-e) Quantification of T cell subsets in mouse lungs from mice vaccinated with BCG or BCG-TetOFF-DL; (a) effector memory CD4 T cells; (b) of effector memory CD8 T cells; (c) CD153 expressing CD4 T cells; (d) lung resident memory CD4 T cells; (e) Cytokine (TNF,  $\text{IFN}\gamma$ , IL2, IL17A) expressing lung cells following ex vivo restimulation with PPD prior to intracellular cytokine staining and Boolean OR gating. Symbols are data from individual mice with lines indicating mean  $\pm$  SD. Two-way ANOVA was performed, and Tukey's adjusted p-values are shown for each time point. \*\*\*\*  $p < 0.0001$ , \*\*\*  $p < 0.001$ , \*\*  $p < 0.01$ , \*  $p < 0.05$ , ns  $p > 0.10$ .

719 (f) Bacterial burden in lungs and spleens of vaccinated and PBS treated mice. Mice were infected with Mtb  
720 H37Rv by aerosol 90 days post vaccination. CFU on day one post infection were  $90 \pm 17$ . Symbols represent  
721 data from individual mice with lines indicating mean  $\pm$  SEM. Two-way ANOVA was performed on  $\log_{10}$ -  
722 transformed data and Tukey's adjusted p-values are shown for each time point. \*\*\*\* p < 0.0001, \*\*\*, p < 0.001,  
723 \*\* p < 0.01, \* p < 0.05, ns p > 0.10.

724  
725 **Figure 4 Discontinuation of doxy limits BCG-TetOFF-DL persistence in NHP.** (a) Persistence study design  
726 (b) Memory CD4+ pre vaccination, memory effector CD4+ 4 weeks post vaccination, memory CD8+ pre  
727 vaccination and memory CD8+ 4 weeks post vaccination (n=3/group) total cell numbers isolated from the BAL,  
728 stimulated with H37Rv WCL. Two-way ANOVA was performed. There were no treatment effects, but total cells  
729 increased over time in all cell types. Median and range shown. (c) Gross pathology scores at necropsy. (d-g)  
730 Bacterial burden (CFU) of BCG-TetOFF-DL CFU recovered from total body of animal (d), thoracic cavity (e),  
731 lungs (f) and thoracic lymph nodes (g) (n=3/group, mean and SD shown). Number of effector CD4+ cells (h) and  
732 CD8+ cells (i) per gram of lung tissue, stimulated with media or H37Rv WCL (average of 4 lung tissues per  
733 animal, n=3 animals/group). Memory is defined as CD45RA+CD28-, CD45RA-CD28+ or CD45RA-CD28-.

734  
735 **Figure 5 BCG-TetOFF-DL provides robust protection against Mtb infection in macaques.** (a) Efficacy study  
736 design. (b, c) Number of lung granulomas over time (b) and at necropsy (c). (d, e) Total lung FDG activity by  
737 PET imaging over time (d) and at necropsy (e). (f) Gross pathology scores at necropsy. (g) Total thoracic  
738 bacterial burden at necropsy. (h) Fisher's exact test showing trend of higher levels of sterility in animals  
739 vaccinated with BCG-TetOFF-DL versus WT BCG Pasteur; Fisher's exact p-value reported. Total bacterial  
740 burden in lungs (i) and thoracic lymph nodes (j). WT BCG (n=8), BCG-TetOFF-DL (n=8) and unvaccinated  
741 animals (n=10). Stars represent historical controls. Lines represent the median and range. Statistic for c, e, f, g,  
742 i, j Kruskal-Wallis tests were performed and Dunn's p-values (adjusted for multiple comparisons) were reported.

743  
744  
745 **Figure 6 BCG-TetOFF-DL induces more CD4 T cells producing cytokines in lung tissue compared to WT**  
746 **BCG.** (a) Frequency of CD4+ and CD8+ T-cells as a percentage of CD3+ cells isolated from homogenized lung

747 tissue at necropsy (WT BCG , BCG-TetOFF-DL n=8, unvaccinated n = 2). Frequency of effector CD4+ and CD8+  
748 T-cells in the lung (b) and thoracic lymph nodes (c) producing cytokines or cytotoxic molecules. Mean with SD  
749 shown. Statistics: Mann-Whitney p values reported comparing BCG-TetOFF-DL and WT BCG.

750  
751  
752  
753  
754  
755 **Figure S1. Single and dual lysin kill switches.** (a) TetON single lysin kill switch schematic. Lysin expression  
756 is repressed by tetracycline repressor (TetR) and induced by anhydrotetracycline (atc) or doxycycline (doxy)  
757 which bind TetR and prevent it from binding DNA.

758 (b) Impact of atc on growth of BCG-TetON single lysin strains. The paper disc contains 1  $\mu$ g of atc.

759 (c) TetOFF dual lysin kill switch schematic. Reverse TetR (Rev TetR) binds to DNA in complex with atc or doxy  
760 to repress D29L. TetR represses PipR and in the presence of atc/doxy PipR is expressed and represses L5L.

761 (d) Impact of atc on growth of BCG-TetOFF-DL. The paper disc contains 1  $\mu$ g of atc.

762  
763 **Figure S2. In vitro characterization of BCG kill switch strains.**

764 (a) Growth of BCG TetON single and dual lysin kill switch strains with and without atc. OD<sub>580</sub> data are means  
765 from duplicate cultures.

766 (b) Western blot analysis of culture filtrates from BCG-TetON-DL and BCG-TetOFF-DL strains grown in the  
767 absence of detergent. A whole cell lysate of WT BCG serves as control. Eno and PrcB were enriched in culture  
768 filtrate of BCG-TetON-DL after 6 and 9 days of growth in the presence of atc and in culture filtrate of BCG-  
769 TetOFF-DL after 6 and 9 days of growth in the absence of atc indicating cell lysis.

770 (c) Expression of two lysins reduces the fraction of escape mutants compared to expression of single lysins.  
771 Cultures were grown in the presence of atc. Symbols represent data from 3-6 individual cultures and means  $\pm$

SD are depicted. Significance was determined by one-way analysis of variance (ANOVA) with Tukey's adjusted p-values shown; \*\*\*\*  $P < 0.0001$ , \*\*\*,  $p < 0.001$ .

(d) Growth of BCG TetOFF single and dual lysin kill switch strains with and without atc. Data are means  $\pm$  SD from triplicate cultures. Error bars are too small to be seen.

(e) Expression of two lysins reduces the fraction of escape mutants compared to expression of single lysins. Cultures were grown in the absence of atc. Symbols represent data from 6 individual cultures and means  $\pm$  SD are depicted. Statistical significance was assessed by one-way ANOVA with Tukey's adjusted p-values shown; \*\*\*\*  $P < 0.0001$ , \*\*\*,  $p < 0.001$ .

### **Figure S3. Survival of BCG, BCG-TetOFF-DL and BCG-TetON-DL following intravenous vaccination.**

(a) CFU from lungs and spleens of mice infected with BCG and BCG-TetOFF-DL not receiving doxy.

(b) CFU quantification from lungs and spleens of mice infected with BCG and BCG-TetON-DL treated with doxy.

Data are means  $\pm$  SEM from 4-5 mice per group and time point.

(c) CFU quantification from lungs and spleens of BCG-TetOFF-DL infected SCID mice treated or not with doxy for the indicated times. Data are means  $\pm$  SD from 4 mice per group and time point.

Multiple unpaired t-tests run on  $\log_{10}$ -transformed data at each time point with Holm-Šídák adjusted p-values shown. \*\*\*\*  $p < 0.0001$ , \*\*\*,  $p < 0.001$ , \*\*  $p < 0.01$ , \*  $p < 0.05$ , #  $0.05 < p < 0.10$ , ns  $p > 0.10$ .

(d,e) Lung sections stained with hematoxylin and eosin from SCID mice infected with BCG-TetOFF-DL for 84 days. (d) Mice were treated with doxy from day 1-14. (e) Mice were treated with doxy from day 1- 84. Each section is from an individual mouse and is representative of each lung.

### **Figure S4. BCG-TetON-DL and wt BCG provide similar protection against Mtb infection in mice.** Mice were i.v. vaccinated with BCG or BCG-TetON-DL or received PBS.

(a,b) Quantification of effector memory CD4 and CD8 T cells in mouse lungs from mice vaccinated with BCG and BCG-TetON-DL. Symbols are data from individual mice with lines indicating mean  $\pm$  SD. Two-way ANOVA

797 was performed with Tukey's adjusted p-values shown for each time point. \*\*\*\*  $p < 0.0001$ , \*\*\*,  $p < 0.001$ , \*\*  $p$   
798  $< 0.01$ , \*  $p < 0.05$ , ns  $p > 0.10$ .

799 (c) Quantification of cytokine producing antigen specific CD4 T cells from mice vaccinated with BCG and BCG-  
800 TetON-DL on day 30 post vaccination. Lung cells were restimulated ex vivo with PPD prior to intracellular  
801 cytokine staining. Two-way ANOVA with Tukey's adjusted p-values shown for each cytokine producing  
802 population. For most of the cytokine producing cells, there were no statistically significant differences among  
803 the treatment groups. \*\*\*\*  $p < 0.0001$ , \*\*\*,  $p < 0.001$ , \*\*  $p < 0.01$ , \*  $p < 0.05$ , ns  $p > 0.10$ .

804 (d) Bacterial burden in lungs and spleens of vaccinated and PBS treated mice. Mice were infected with Mtb  
805 H37Rv by aerosol 90 days post vaccination. Symbols represent data from individual mice with lines indicating  
806 mean  $\pm$  SEM. Two-way ANOVA performed on  $\log_{10}$ -transformed data with Tukey's adjusted p-values shown at  
807 each time point. \*\*\*\*  $p < 0.0001$ , \*\*\*,  $p < 0.001$ , \*\*  $p < 0.01$ , \*  $p < 0.05$ , ns  $p > 0.10$ .

808  
809 **Figure S5 Histologic analysis indicates microgranulomas in spleen, liver and lymph nodes 8 weeks post-**  
810 **BCG-TetOFF-DL.** H&E staining of fixed spleen (a), lymph node (b) and liver (c) tissue. (d) Spleen size at  
811 necropsy for macaques in persistence study and macaques vaccinated and challenged with Mtb. Dashed lines  
812 represent normal spleen size range of adult male MCMs. (d, e) Lymphocyte composition of lung tissue (e, n=4)  
813 and thoracic lymph nodes (f, n=3) from NHP in persistence study at necropsy.

814  
815 **Figure S6 T cell responses in airways are similar between BCG-TetOFF-DL and WT BCG after**  
816 **vaccination.** Total number of cells, CD4+, CD8+, effector memory CD4+ and CD8+ cells during the vaccination  
817 phase with BCG-TetOFF-DL, WT BCG or unvaccinated macaques. BAL samples were obtained pre-vaccination  
818 and 4, 12, 20 weeks post vaccination and stimulated with Mtb WCL. Flow cytometry was performed with  
819 intracellular staining for effector molecules IFN- $\gamma$ , TNF, IL-17, IL-2, GzmB, GzmK, granulysin or perforin  
820 (vaccinated groups n=8, unvaccinated n=2). Multiple unpaired t-tests were used to compare groups at each time  
821 with Holm-Šídák adjusted p-values ( $\# 0.05 < p < 0.10$ ). Median and IQR shown.

822

823 **Figure S7 Individual effector molecules produced by T cells in lungs of vaccinated and challenged NHP.**

824 Total number of CD4+, CD8+, effector memory CD4+ and CD8 $\alpha\beta$ + cells in the lung at necropsy (vaccinated  
825 groups n=8, unvaccinated n=2). Cells producing either cytokines or cytotoxic molecules (IFN- $\gamma$ , TNF, IL-17, IL-  
826 2, GzmB, GzmK, granulysin or perforin) were analyzed. Mann-Whitney p-values reported. Median shown  
827 .

828 **Figure S8 Splenomegaly reduces over time post IV-BCG vaccination**

829 Spleen size at necropsy for macaques in persistence study and macaques vaccinated and challenged with Mtb.  
830 Dashed lines represent normal spleen size range of adult male MCMs.

831

832 **Figure S9 Gating strategy for flow cytometry**

833 **Table S1: Flow cytometry panel for NHP samples in persistence study**

834 **Table S2: Flow cytometry panel for NHP samples in protection study**

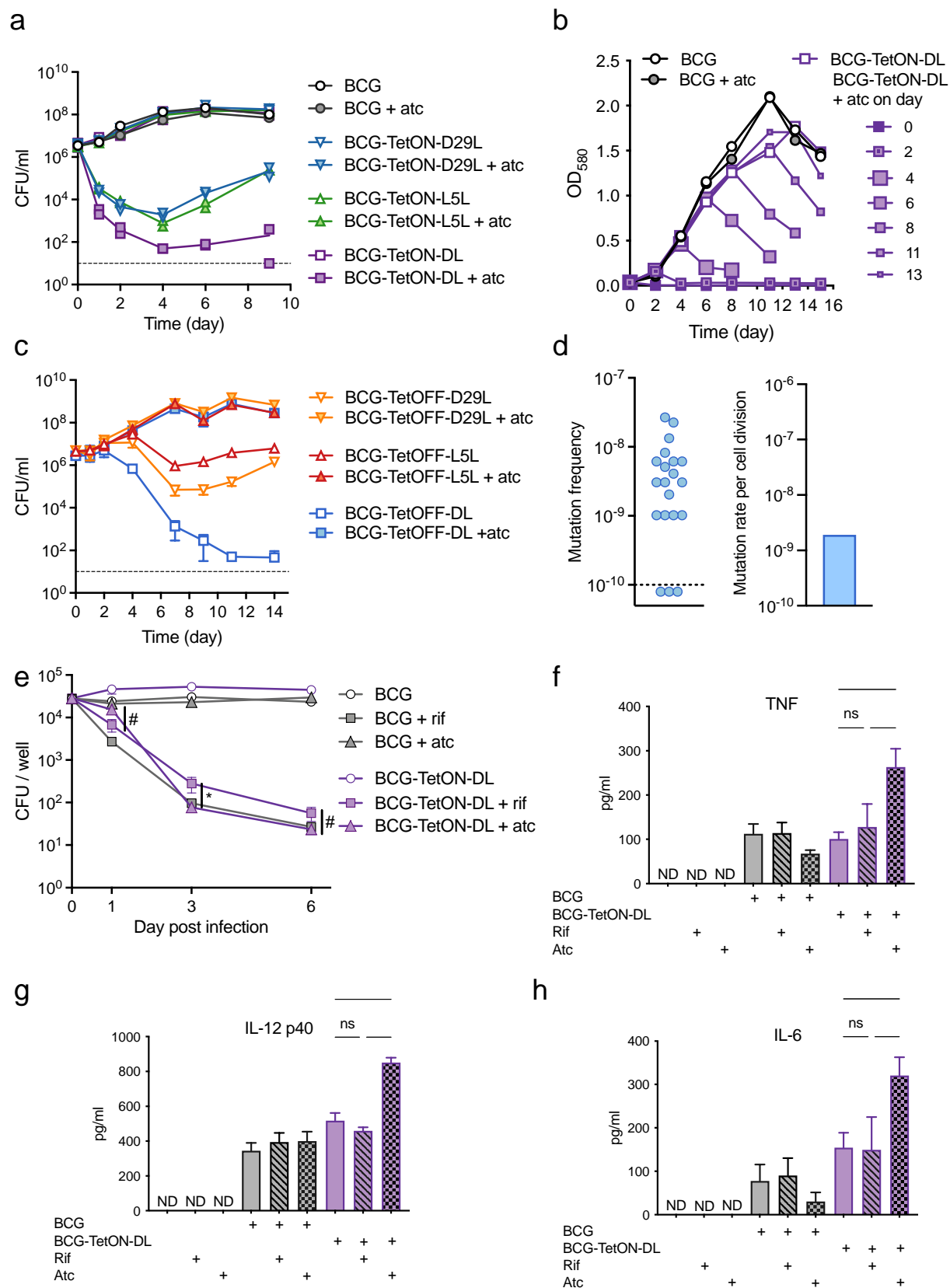
835 **Table S3 Full details on macaques used in this study**

836

837

838

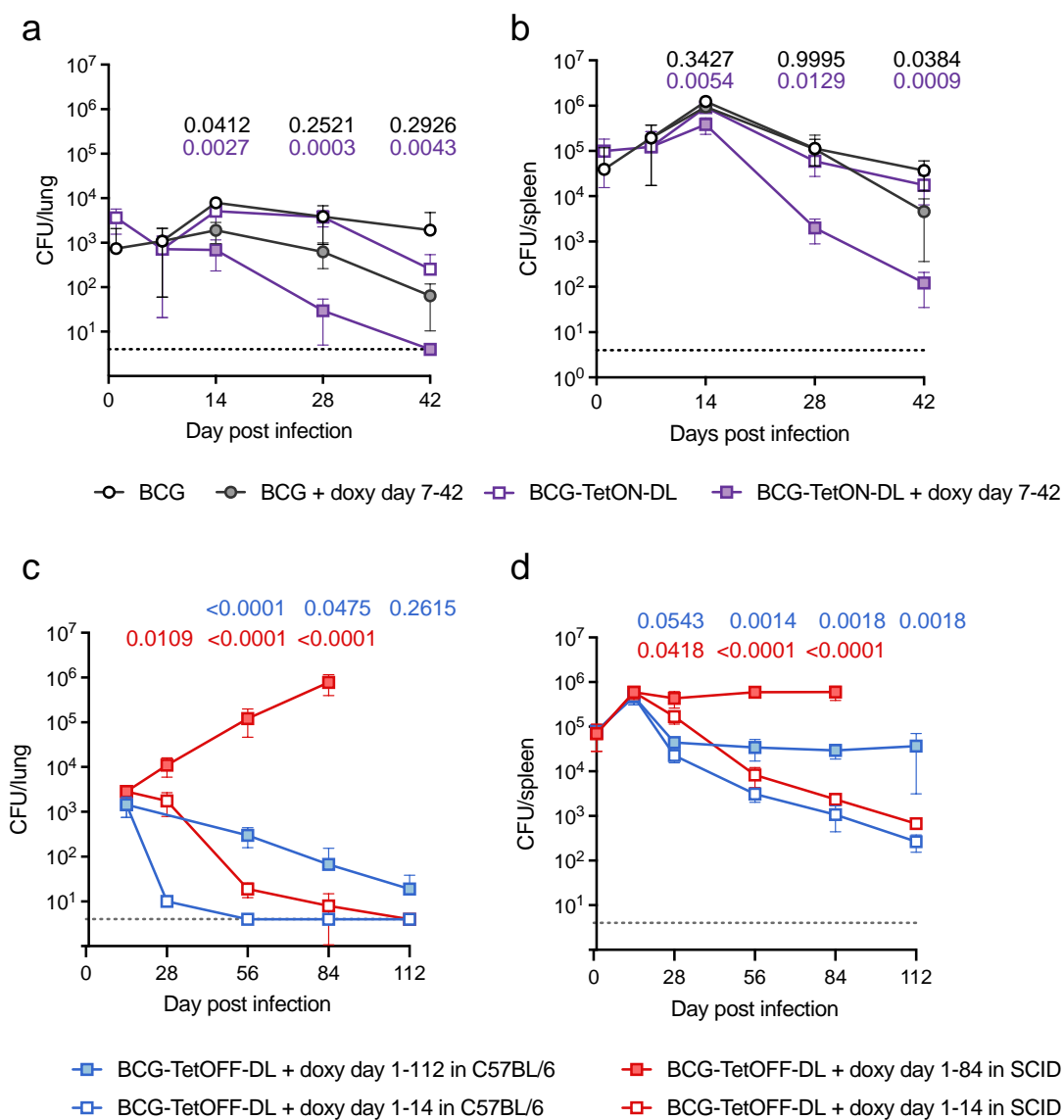
839



840

841 **Figure 1**

842



843

844

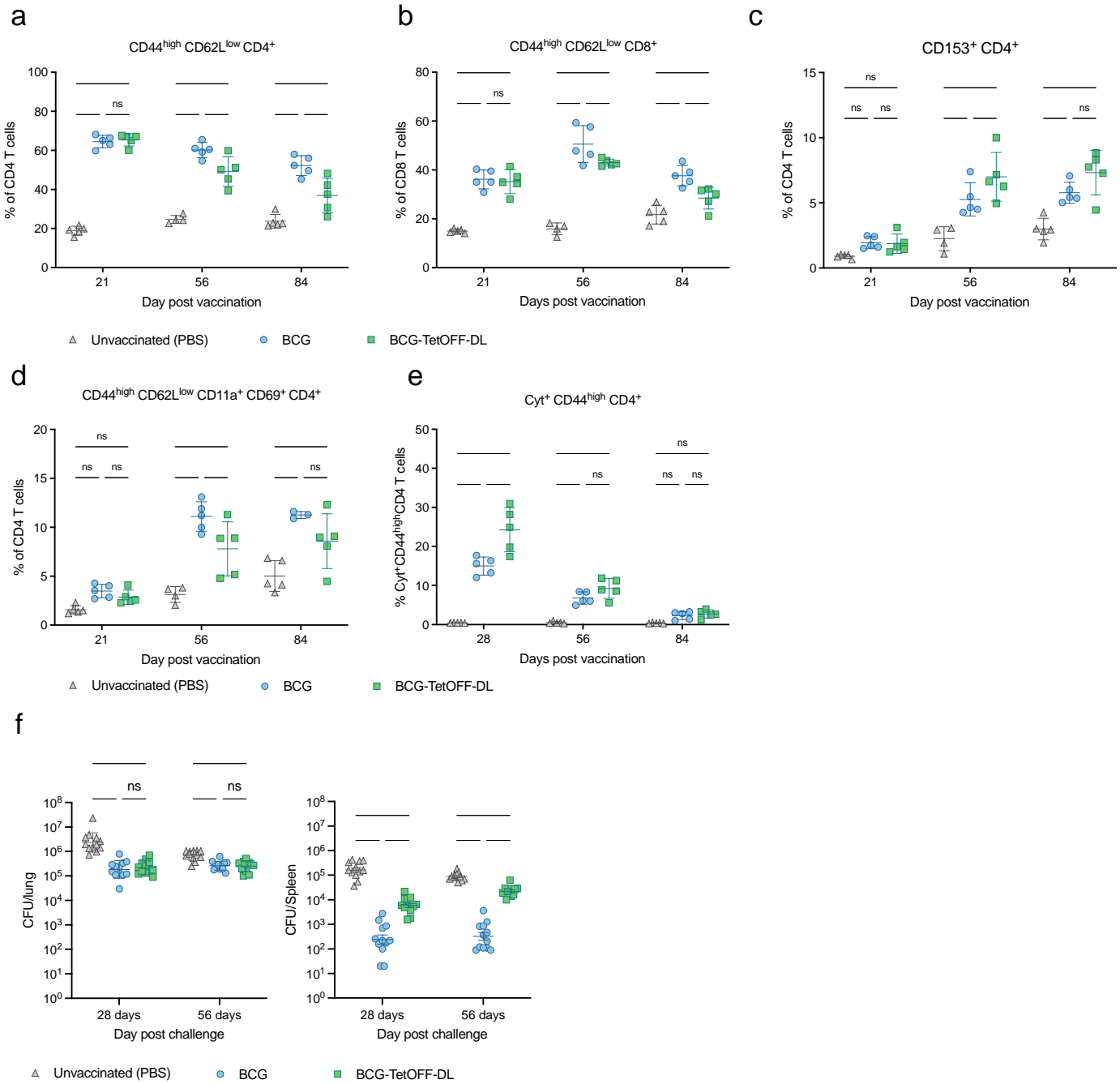
845

846

**Figure 2**



847



848

849

850

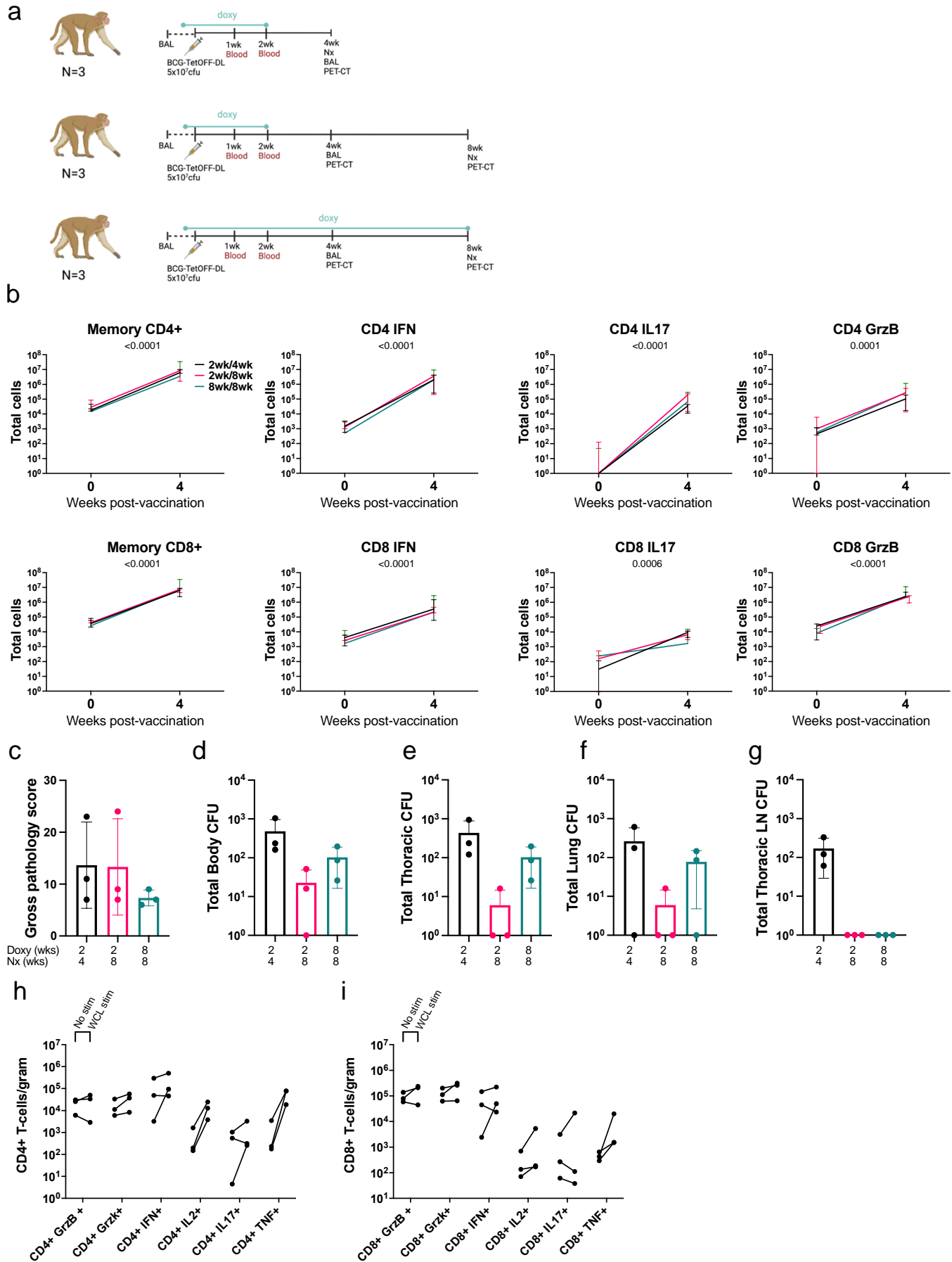
851

**Figure 3**

852

853

854

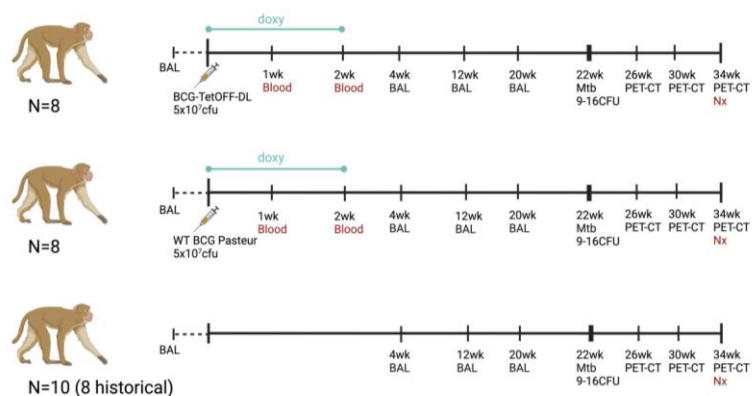


855

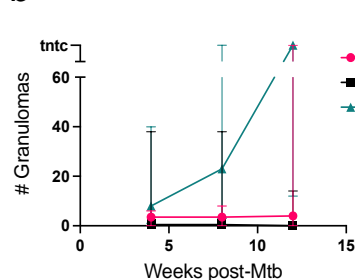
856

Figure 4

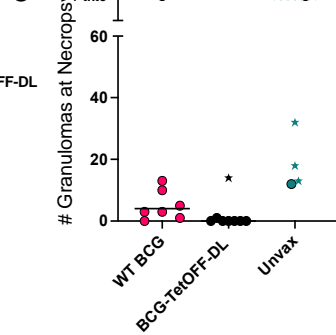
a



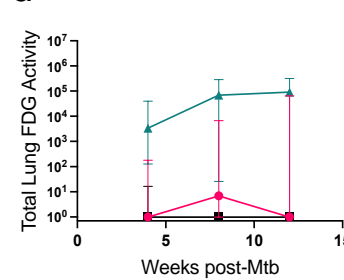
b



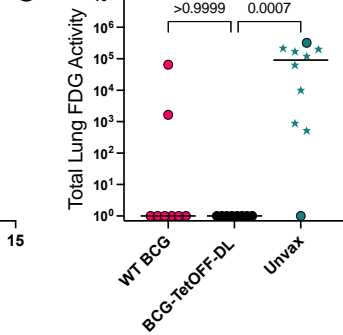
c



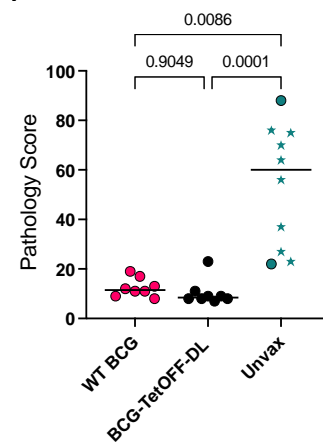
d



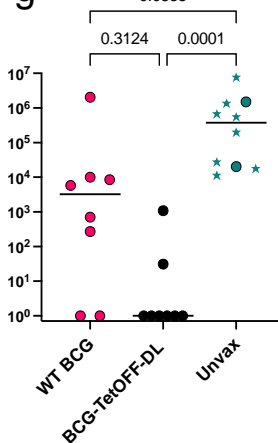
e



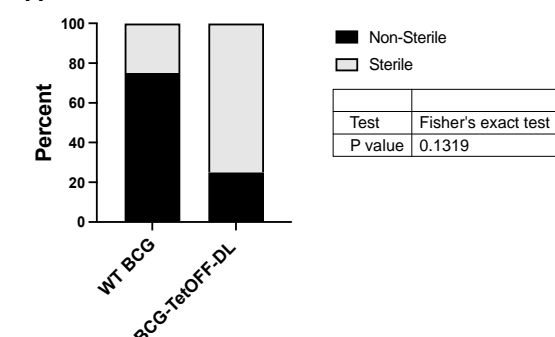
f



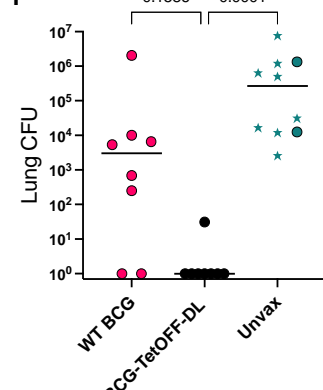
g



h



i



j

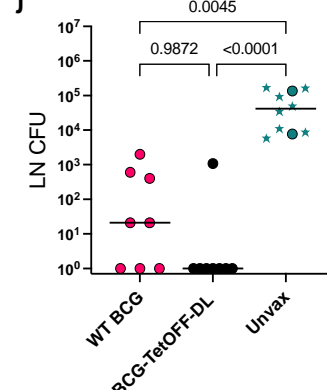
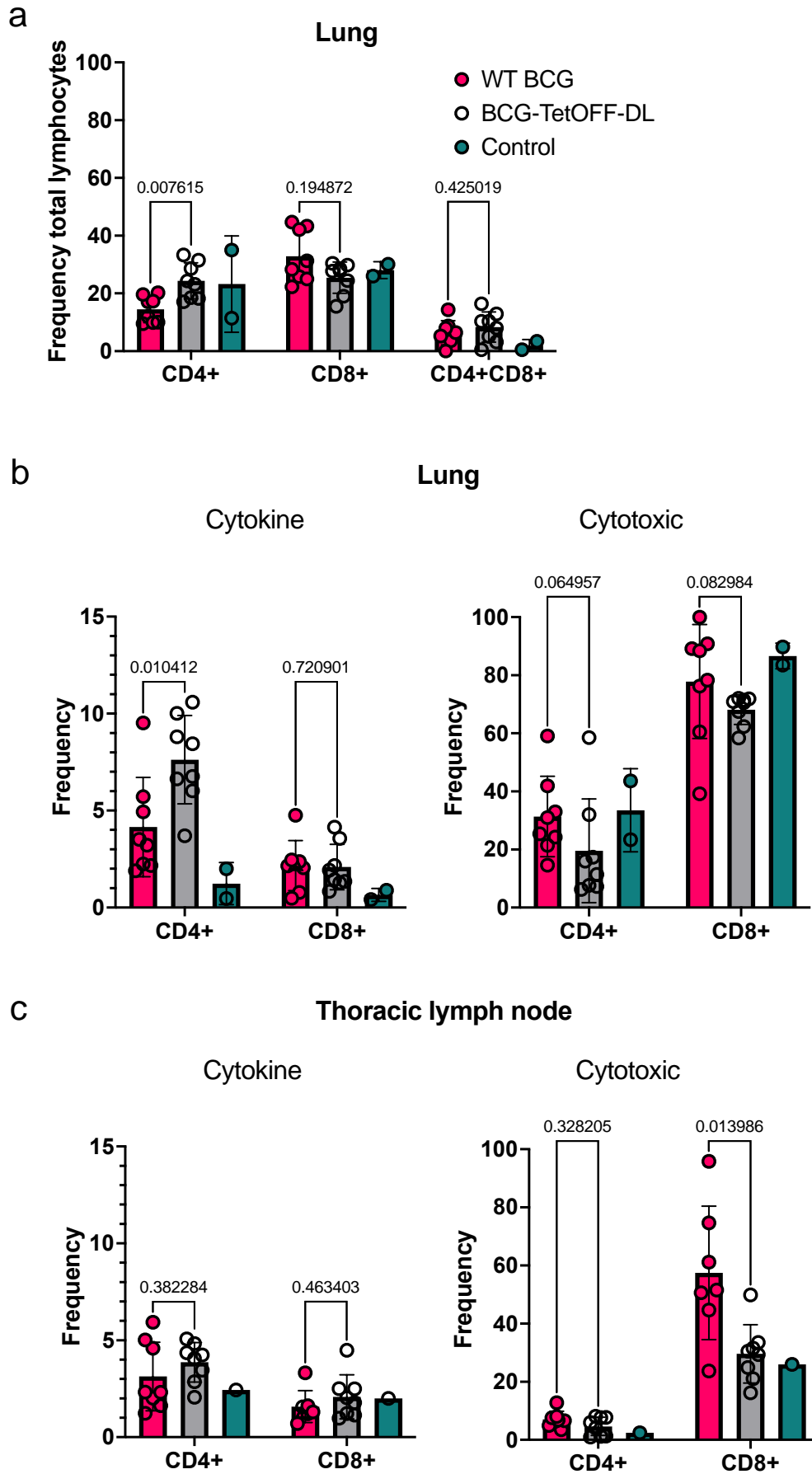


Figure 5



885

886

Figure 6

887

888

889